NASA Contractor Report 182182

DEVELOPMENT OF A 39.5 GHz KARP TRAVELING-WAVE TUBE FOR USE IN SPACE

FINAL REPORT

A. Jacquez and D. Wilson

Varian Associates, Inc.
Palo Alto, California

October 1988

Prepared for
NASA-Lewis Research Center
Cleveland, OH 44135
Under Contract NAS3-23259

National Aeronautics and
Space Administration

Lewis Research Center
Cleveland, Ohio 44135
AC 216 433-4000

PREFACE

The work reported herein was supported by NASA-Lewis Research Laboratory on Contract NAS3-23259 under the direction of James Dayton and Frank Kavanagh. This work was performed by members of the Varian Helix Engineering Department. The authors wish to thank all of those who participated in this effort, especially D.T. Andker and J.L. Nolan.

TABLE OF CONTENTS

PRECEDING PAGE BLANK NOT FILMED

LIST OF ILLUSTRATIONS

LIST OF ILLUSTRATIONS (Cont'd)

1.0 INTRODUCTION

1.1 GENERAL INFORMATION

The purpose of this program was to design, fabricate and test a traveling-wave tube (TWT) capable of operating at 39.5 GHz, with a small-signal bandwidth of at least one percent, and a power output of at least 200 W CW, for potential use in a space-borne communications satellite amplifier. The most promising circuit for this application is a derivative of a concept developed several years ago by Arthur Karp,[1] and hence is referred to as a Karp slow-wave circuit. This particular circuit consists of one or more ladder-like, but not necessarily planar, arrays of conductors, arranged within an axially uniform enclosure that is typically a single- or double-ridged waveguide. The Karp slow-wave structure is a potentially inexpensive alternative to the conventional coupled-cavity slow-wave circuit for high-average-power, millimeter-wave applications. The potential for cost reduction arises because the ladder and the outer shell or enclosure are fabricated separately, permitting the employ of a variety of techniques, not conventionally applied to tube manufacture. Upon assembling a Karp circuit-tube, only a few relatively large parts are brazed. This fabrication procedure is in sharp contrast to a conventional coupled-cavity TWT, in which hundreds of superbly machined parts must be brazed to form the slow-wave circuit.

Prior to the initiation of this program, the Karp slow-wave circuit was analyzed as a fundamentally forward-wave amplifier in a theoretical study performed at NASA-Lewis Research Center.[2] The principal results of this analysis were then verified at Varian under Contract NAS3-21930. That program also verified the feasibility of producing a Karp Circuit TWT capable of an output of hundreds of watts at a bandwidth of a few percent in the millimeter-wave frequency band.[3]

Tasks undertaken in the course of this program included:

— Design, fabrication, and testing of a scale-model cold-test structure of the Karp slow-wave circuit. This work provided the basis for the subsequent design of a 39.5 GHz circuit intended to produce 200 W CW over at least a one percent bandwidth.

— Experiments on innovative fabrication techniques often not previously applied to the design of microwave tubes.

— Design of a laboratory model tube. This work included original design of the circuit, waveguide coupling, magnetic focusing, and mechanical support structures, as well as adaptation of existing cathode and collector designs.

— Fabrication of a laboratory model tube, including all major subassemblies. This work included successfully brazing circuit assemblies 70% longer than any previously assembled.

1.2 BACKGROUND HISTORY

In the early 1950s, the thin, flat ladder was recognized as a practical periodic element at millimeter wavelengths, provided one could invent a slow-wave interaction circuit incorporating it.[1,4]

The first ladder-based slow-wave circuit studied was a plain, rectangular waveguide with the ladder installed in the broad wall. The rung span was less than the waveguide breadth.[5] Slow-wave propagation was achieved over a useful bandwidth extending downward from the half-wave resonance frequency of the rung. The bandwidth became greater yet when a ridge was introduced within the waveguide.[6] The propagation was "forward wave" and the bandwidth depended on both the ridge-to-ladder capacitance and the space available for loops of rf magnetic field to expand beyond the rung anchor points.

During this period and beyond, a single ridge plus a thin, flat ladder combination appeared in low-voltage tubes — primarily backward-wave oscillators (BWOs) for frequencies up to 300 GHz.[7-9] In these designs, the disposition of metal around the rung anchor points varied,[10] hence the bandwidth contribution relative to that from the ladder-to-ridge capacitance was not constant.[11] The current desire for higher power levels requires that the rungs be anchored directly and perpendicular to flat, solid walls to maximize rung cooling,[12] so that the bandwidth must be determined solely by the ridge capacitance. Most analytic efforts to model the structure's field and impedances stipulated extensive flat walls normal to the array of rungs.[12-15] Beam voltages of, at most, a few kilovolts were characteristic of millimeter-wave tubes in the 1950s and early 1960s. In order to avoid an unreasonably fine ladder pitch, only space-harmonic interaction was considered at these low-beam velocities. The beam-wave phase shift per period was between π and 2π for a BWO and 2π to 3π for an amplifier.

Thus the first point made in H.G. Kosmahl's 1978 presentation was that the tens-of-kV beam voltages favored today would permit nonspace-harmonic operation at millimeter wavelengths of a "forward-wave" ladder-based amplifier with a relatively coarse pitch.[15]

"Fundamental/forward" TWT interaction implies per se a relatively high gain/inch, but Kosmahl's second point was that the gain rate would benefit further from the high interaction impedance associated with the ladder. This impedance is due, in part, to the rung resonance at the frequency close to the operating frequency and the consequent high dispersion and low group velocities. These properties also predict a rather narrow "hot" bandwidth which might, however, be acceptable for certain applications.

The principles above led to the previous study programs[3,16] and to the present development program. In these study programs, prior to devising and evaluating TWT designs that were practical embodiments of Kosmahl's principles, some cold-test experimentation with an intentionally simplified slow-wave structure was done. These experiments showed the effects of dimensional changes in a geometry featuring the basic structural elements — rungs, ridge and side walls (see Figure 1). Other tests included measurements of the effects of double ridges on the ω–β curve and interaction impedance.

The move from the earlier space-harmonic and low-power approaches to the forward/fundamental approach and high power for millimeter wavelengths created a very different situation. Beam power densities on the order of a few MW/cm^2 were necessary and pencil-beam optics were the only means for making this manageable from the viewpoint of both the gun and the interaction structure. On the interaction structure side, a low percentage interception is consistent with having a pencil beam in a round "tunnel." On the gun side, a conventional axisymmetric gun, sufficiently convergent to avoid undue cathode loading, permitted the requisite 100 A/cm^2 or more of beam current.

The simple ladder-plus-ridge design is shown on the left side of the illustration in Figure 1. The ladder is then formed and doubled to allow the passage of a pencil beam; and to increase thermal capacity for handling beam interception, there is thermal anchoring to dielectric posts. The forming of the ladder produces a non-circular tunnel for the beam. This design provides thermal paths through the dielectric posts to the ridges for beam-interception heating localized where the rungs are closest to the beam. RF heating in the runs occurs mainly near the side walls to which there is a direct connection.

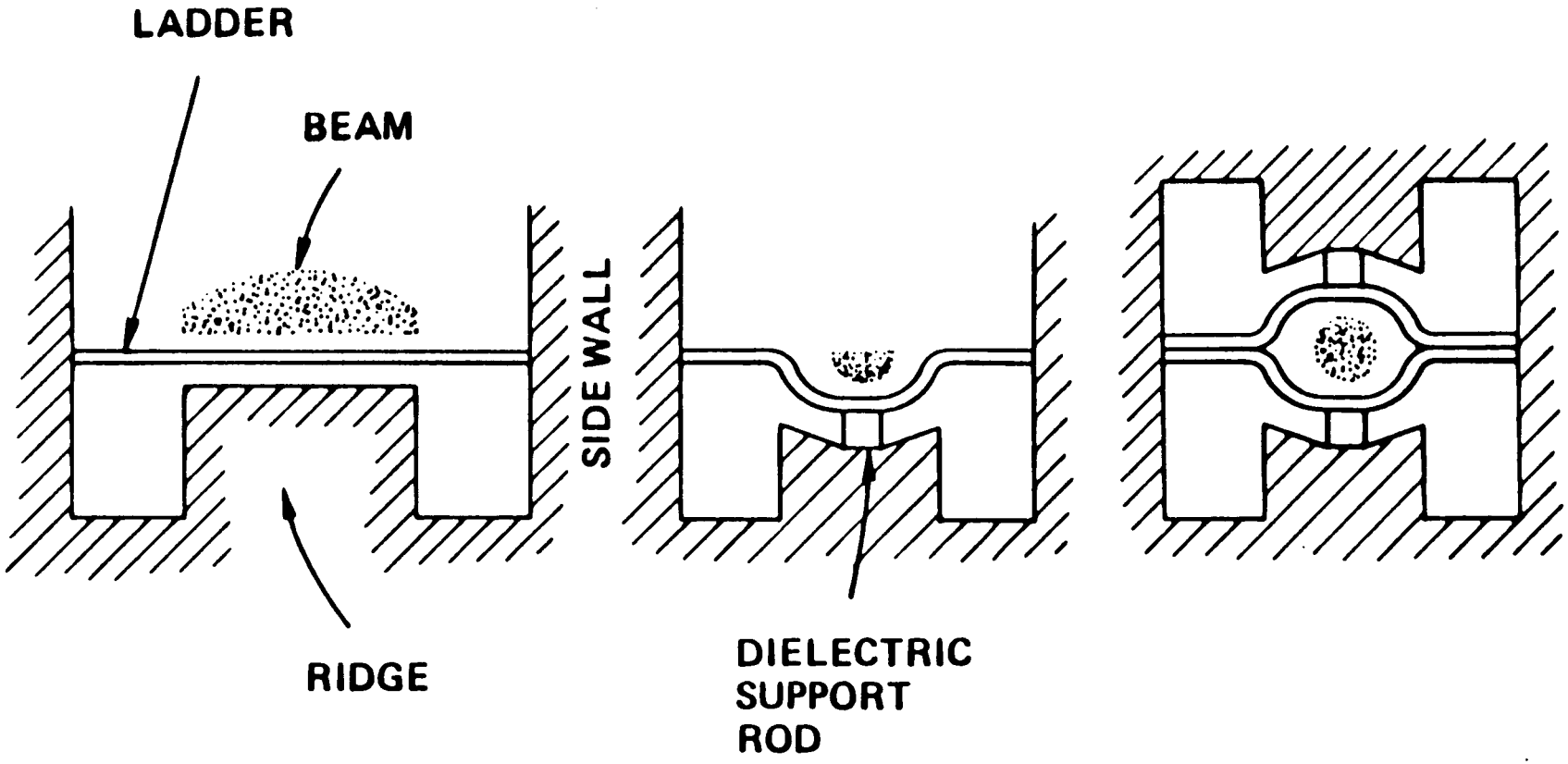

FIGURE 1. FLAT SINGLE LADDER TO "TUNNELADDER" DESIGN

D2623
F1118

These ideas underlay the basic "TunneLadder" interaction structure shown on the right side of the illustration in Figure 1, with two ridges and a ladder assembled from two identical components. As stated, the shaping of the ladder halves provides a more or less oval beam tunnel (with beam interception occurring predominantly at the two positions where heat can travel directly outward through the dielectric support rods). The double-ridge system now does permit propagation of a mode which is TE at the lowest propagating frequency and whose fields are antisymmetric with respect to the latter — in addition to the desired mode which is similarly TE-derived but symmetric with respect to the ladder. With the new ladder-half shaping, the passband upper edge for the desired (symmetric) mode is lower than if the rungs were straight, requiring inward adjustment of the enclosure side walls. However, the passband upper edge for the antisymmetric mode is considerably and safely higher — by the ratio of the total rung length to half the circumference of the more or less oval tunnel.

The dielectric supports proposed are of high-thermal-conductivity Type IIA diamond, nominally 0.25 mm square in cross section. The copper of the ladder rungs and ridges is zirconium doped to effect a strong thermocompression bond to the diamond without risk of contaminating nearby exposed diamond surfaces. Details relating to these supports and the bonding are given in Section 3. The information in this section is also presented in almost the same form in an earlier report.[16]

2.0 COLD TEST

2.1 CIRCUIT COLD TEST

The actual circuit design resulted from cold-test experiments with a 12.5 times scaled model of a 39.5 GHz circuit whose geometry was determined from the results of previous NASA Contract NAS3-21930. A photograph of the cold-test structure is shown in Figure 2. The interaction structure used two shaped ladder elements, each supported by diamond cubes brazed to half of a double-ridge waveguide. Two symmetrical halves were mated, forming a TunneLadder circuit with its two sets of diamond cube supports in a double-ridge waveguide. The prior NASA contract also established that the dielectric cubes would be made from Type IIA nonsynthetic gem-quality diamond because of its exceptionally high thermal conductivity, as shown in Figure 3.

The cold-test model for this program was based on the prior NASA model. The tube was to use:

- Formed ladders made by chemical milling.
- Type IIA diamond support cubes.
- Amzirc alloy for active brazes to the ladder rungs and waveguide ridges.

However, the scale model used Stycast to represent the diamond cubes and machined copper for the chemically milled Amzirc ladders. The rest of the cold-test model was of aluminum. Parts of the waveguide sidewalls were movable to establish the frequency band. Sidewall dimensions were the same in the final waveguide design to simplify parts and subassembly fabrication.

The ω–β diagram for a typical TunneLadder circuit, showing the most significant modes, is shown in Figure 4.

Before beginning cold testing, the decision was made to use the same diamond and ladder dimensions on this program as were already used on the 29 GHz TunneLadder developed on NASA Contract NAS3-22445. In addition, the dimensions of the waveguide ridge were scaled from the work done on a 42 GHz circuit (Contract NAS3-21930). On the basis of comparisons between predicted and actual performance on the 29 GHz tube, a set of operating parameter values were established for the 39.5 Ghz tube. These values are described in detail in Section 4. The beam voltage of 21.7 kV yields a normalized beam

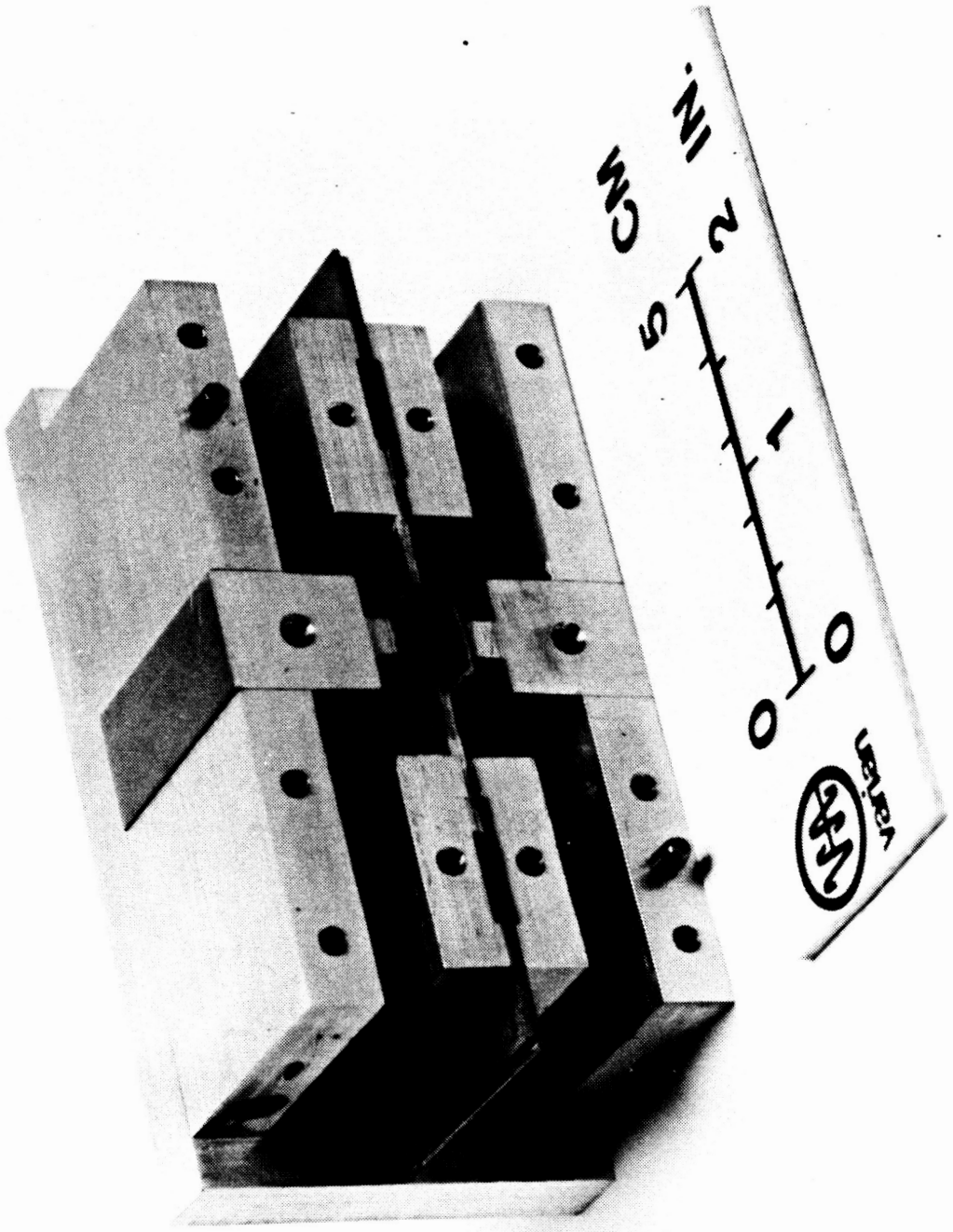

FIGURE 2. COLD-TEST STRUCTURE

F1118

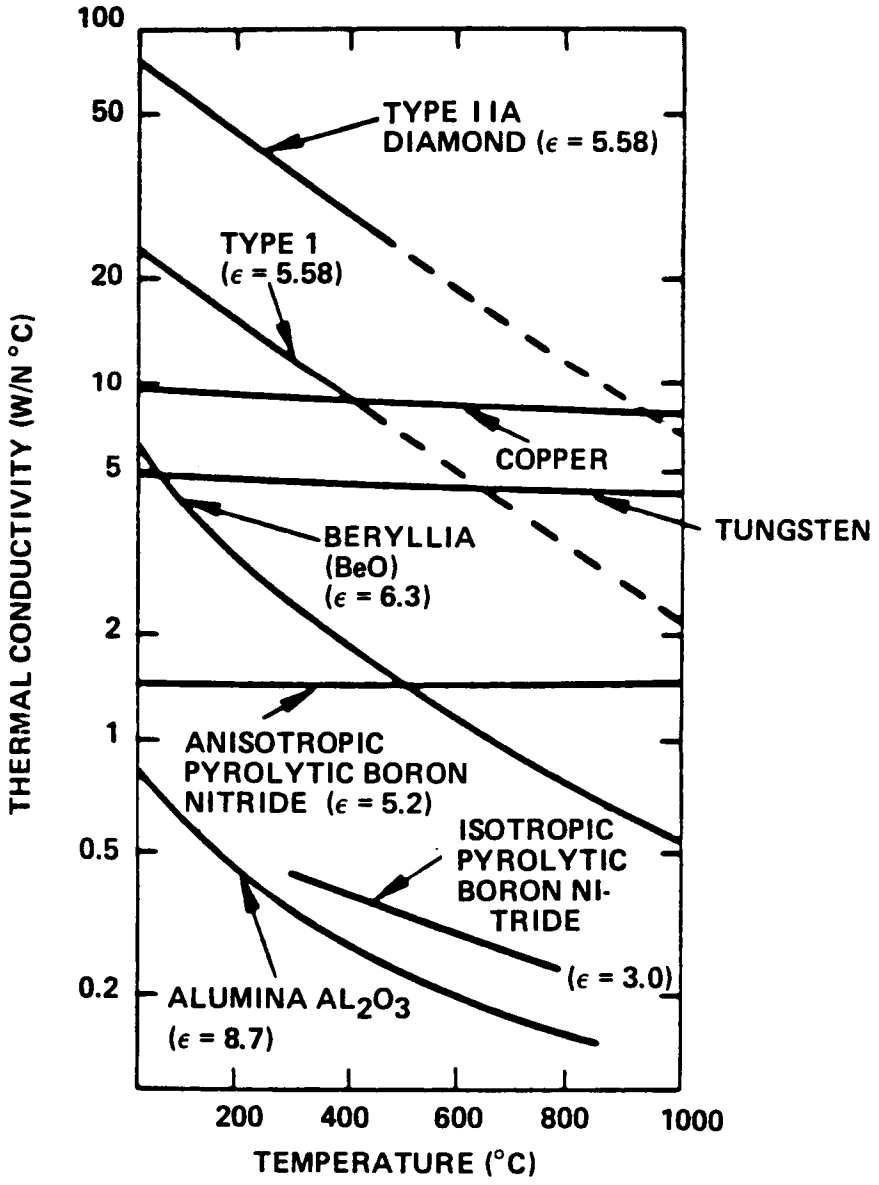

FIGURE 3. THERMAL CONDUCTIVITIES OF CIRCUIT SUPPORT MATERIALS

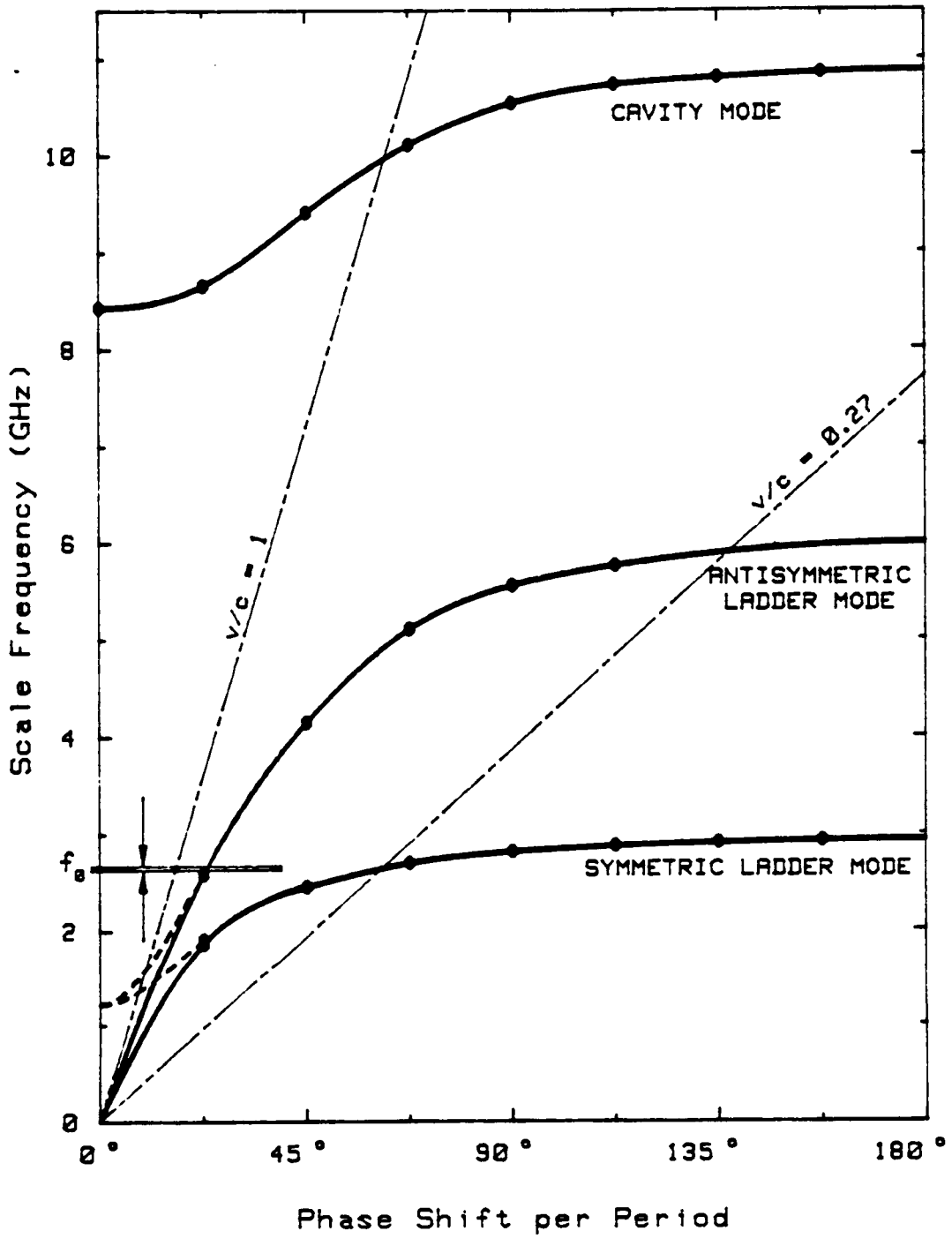

FIGURE 4. ω - β DIAGRAM FOR TYPICAL "TUNNELADDER" CIRCUIT

velocity (v/c) of 0.28. The scale factor of 12.5 gives a scaled frequency of 3.16 GHz. These values are used to determine the remaining circuit dimension, and the waveguide width, as shown in Figures 5 and 6. As can be seen, the wall can be either free or connected to the rest of the waveguide. In the former case, the lower cutoff is dc, but even with a constant wall width (and commensurately higher low frequency band edge) the operating band circuit behavior is relatively unaltered. In Figure 7, the cold-test performances of the 29 GHz and 39.5 GHz cold-test circuits are compared. Figure 8 gives the cold-test velocity and beam-circuit interaction impedance for the 39.5 GHz cold-test circuit. On the basis of this information, the small-signal gain computer program was used to produce the curves shown in Figures 9, 10 and 11. The final dimensions of the cold-test model are given in Figure 12. These computer results indicate a gain per unit length of 28.6 dB/in, which results in a slightly longer circuit than originally anticipated. Nonetheless, the actual focusing and circuit designs, discussed in Sections 4.2 and 4.3 respectively, indicate that this limitation can be accounted for without a major effect on the tube dimensions.

2.2 WAVEGUIDE TRANSITION

The waveguide/circuit transition was scaled directly from the 29 GHz design, using the relative waveguide widths as a scale factor (0.224/0.280 = 0.800). The 29 GHz scaled circuit model is shown in Figure 13. The scaled waveguide-transition model is shown with it in Figure 14.

The final cold-test coupler design is shown in Figure 15, including the dimensions of the coupler tuning elements: inductive iris, capacitive post and reduced-height waveguide short. After optimizing the tuning elements of the transition, the result of this matching effort is shown in Figure 16.

The VSWR for the 29 GHz transition is better than 1.6:1 over a 5% bandwidth and better than 2:1 over a 10% bandwidth. This is more than satisfactory for the expected 1 to 3% "hot" bandwidth. It should be possible to achieve a maximum VSWR better than 2:1 for the actual 39.5 GHz circuit, even with a double-ended matched circuit as implemented for the first models. The only other cold-test experiments were undertaken after later work showed that the diamond cubes would have to have metalized caps to accomplish brazing to the Amzirc ladder rungs. These tests forecast a 2 to 5% lowering of the operating frequency band, as later verified in actual tube tests.

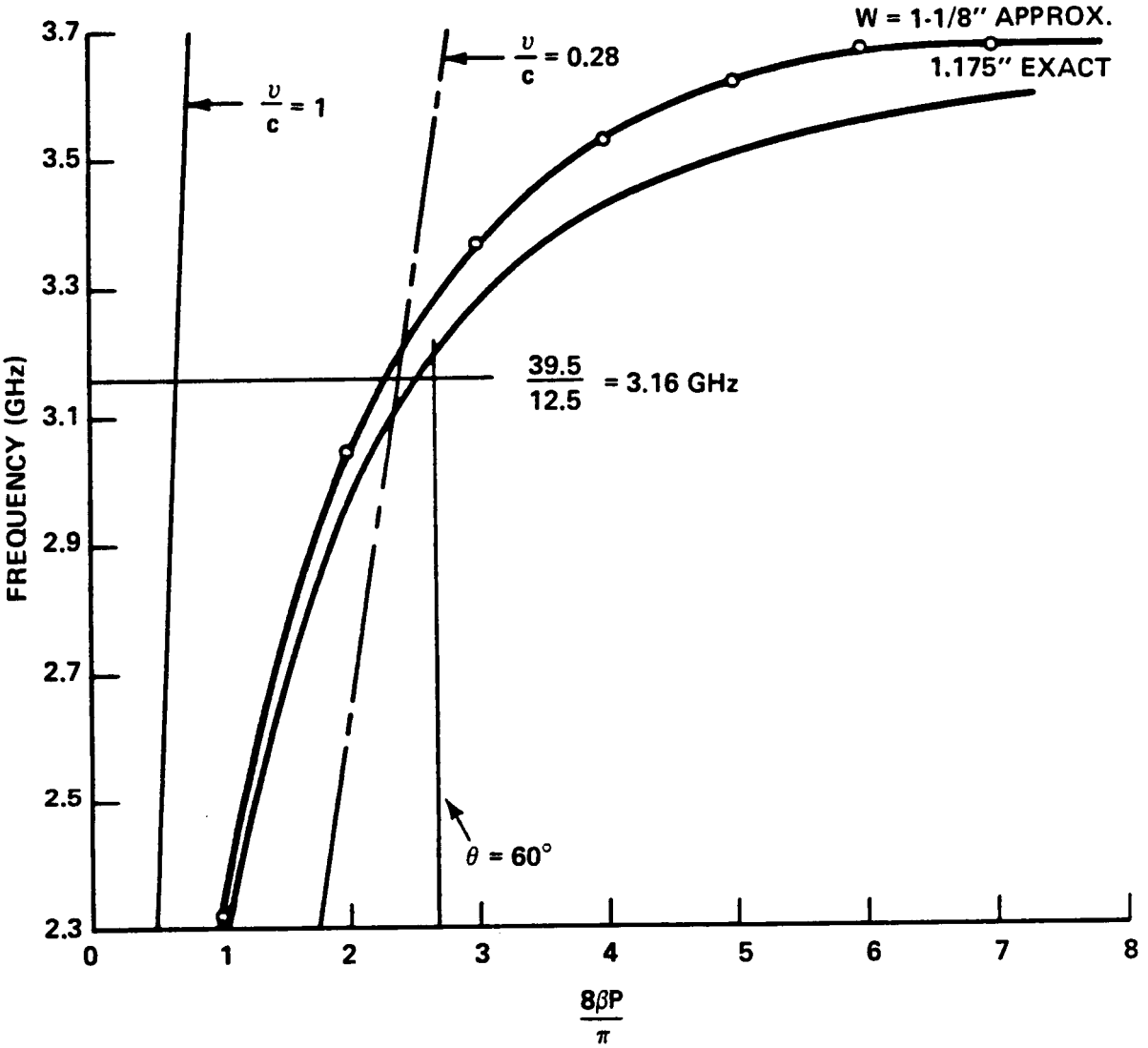

FIGURE 5. SCALED COLD TEST FOR 39.5 GHz TUNNELADDER

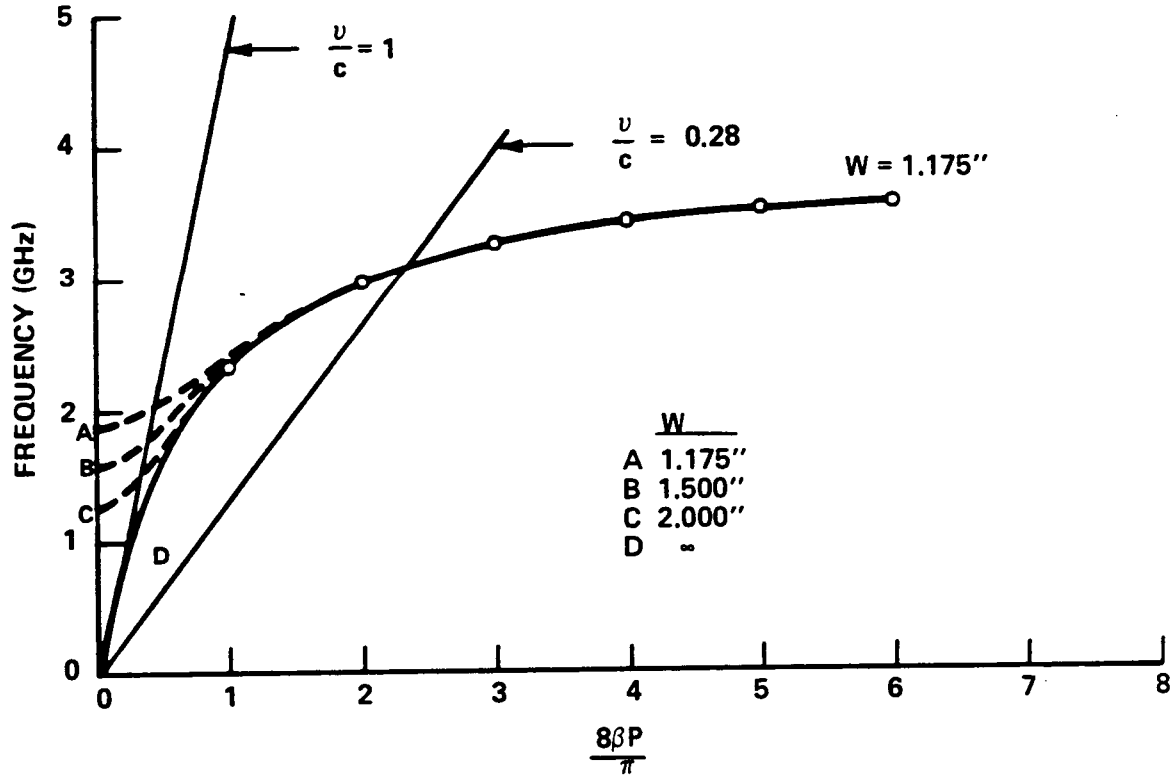

FIGURE 6. EFFECT OF SIDEWALL POSITION ON PASSBAND

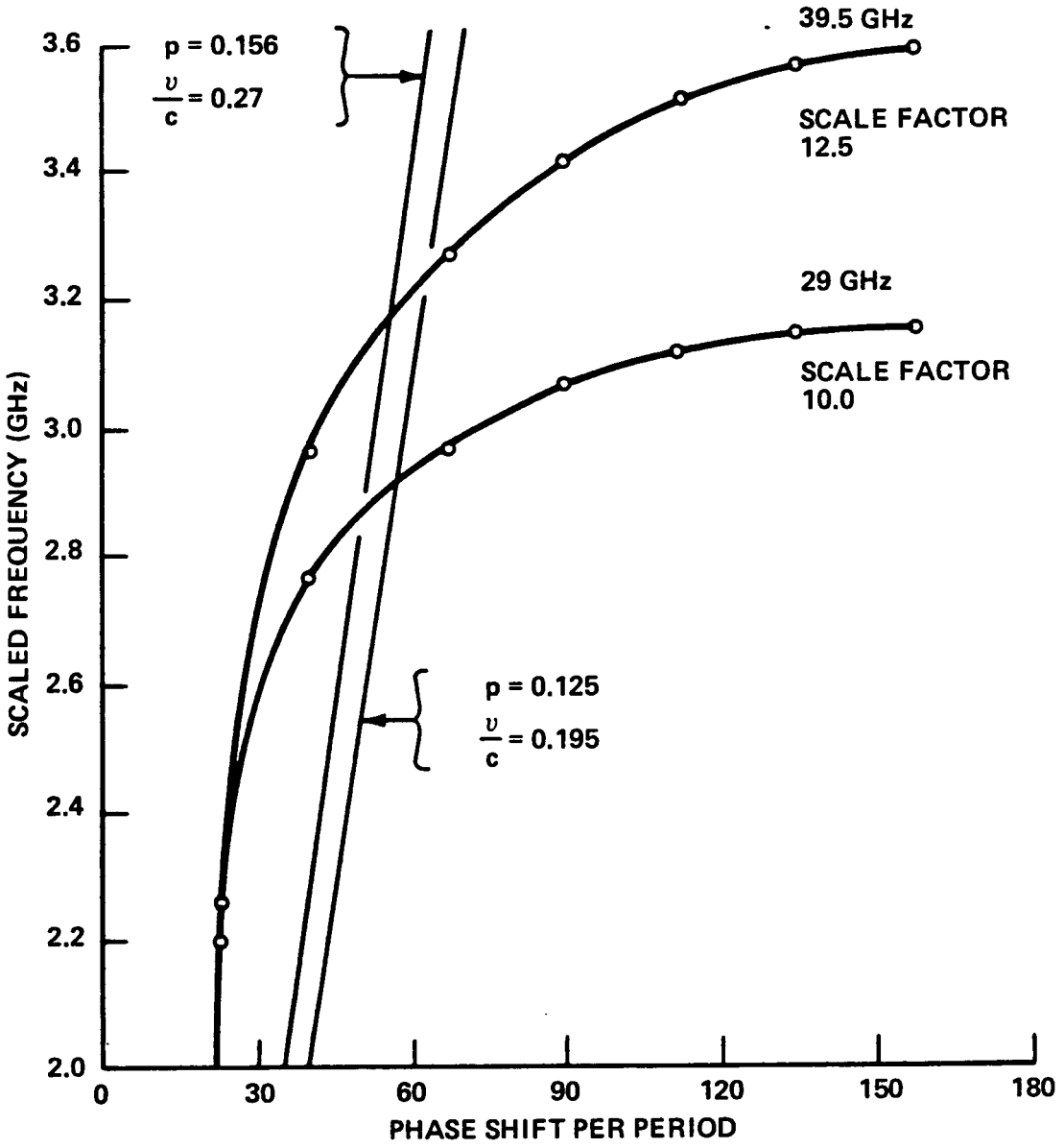

FIGURE 7. AMPLIFIER-PASSBAND ω-β CURVES FOR COLD-TEST CIRCUIT MODELS

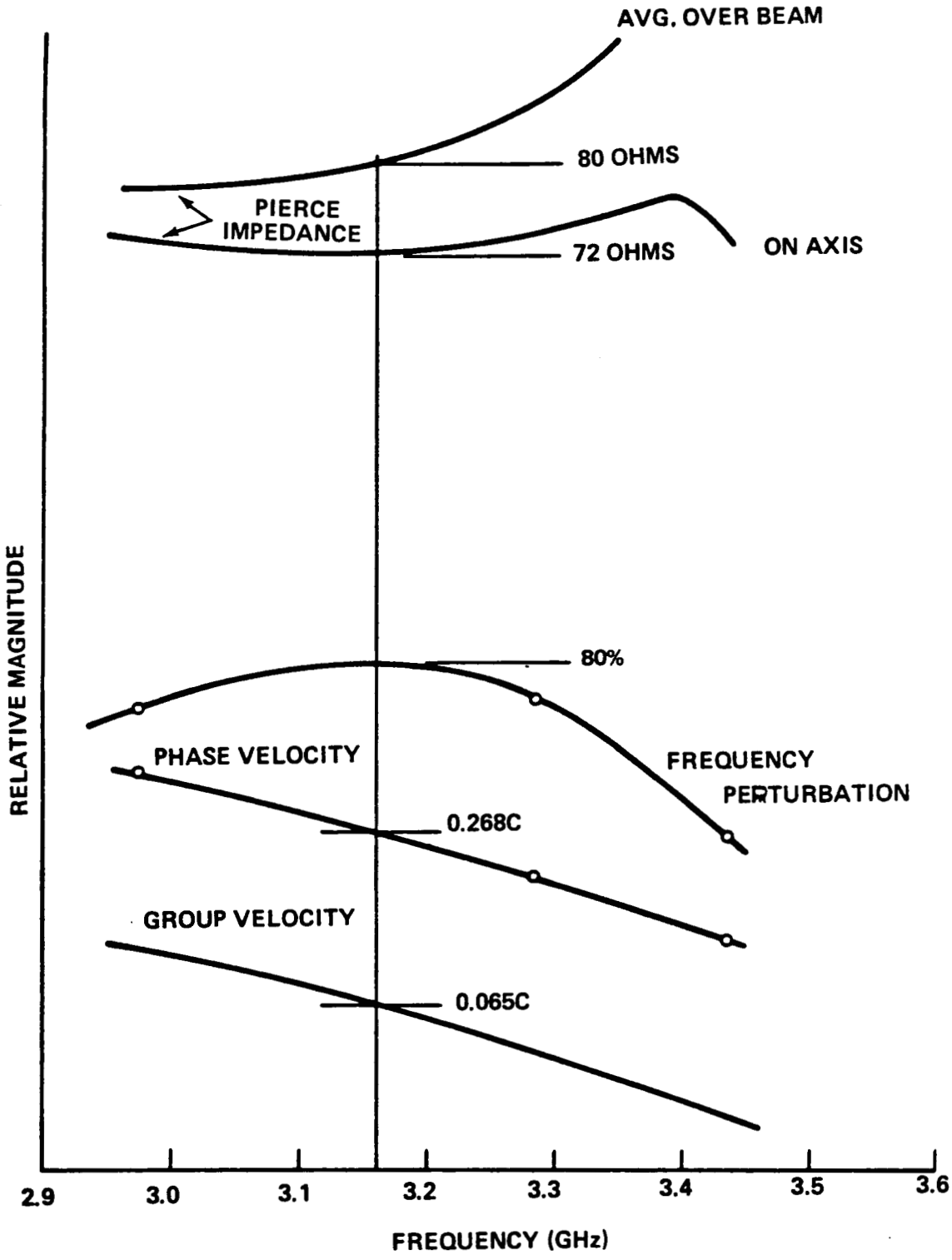

FIGURE 8. COLD-TEST CIRCUIT PERFORMANCE

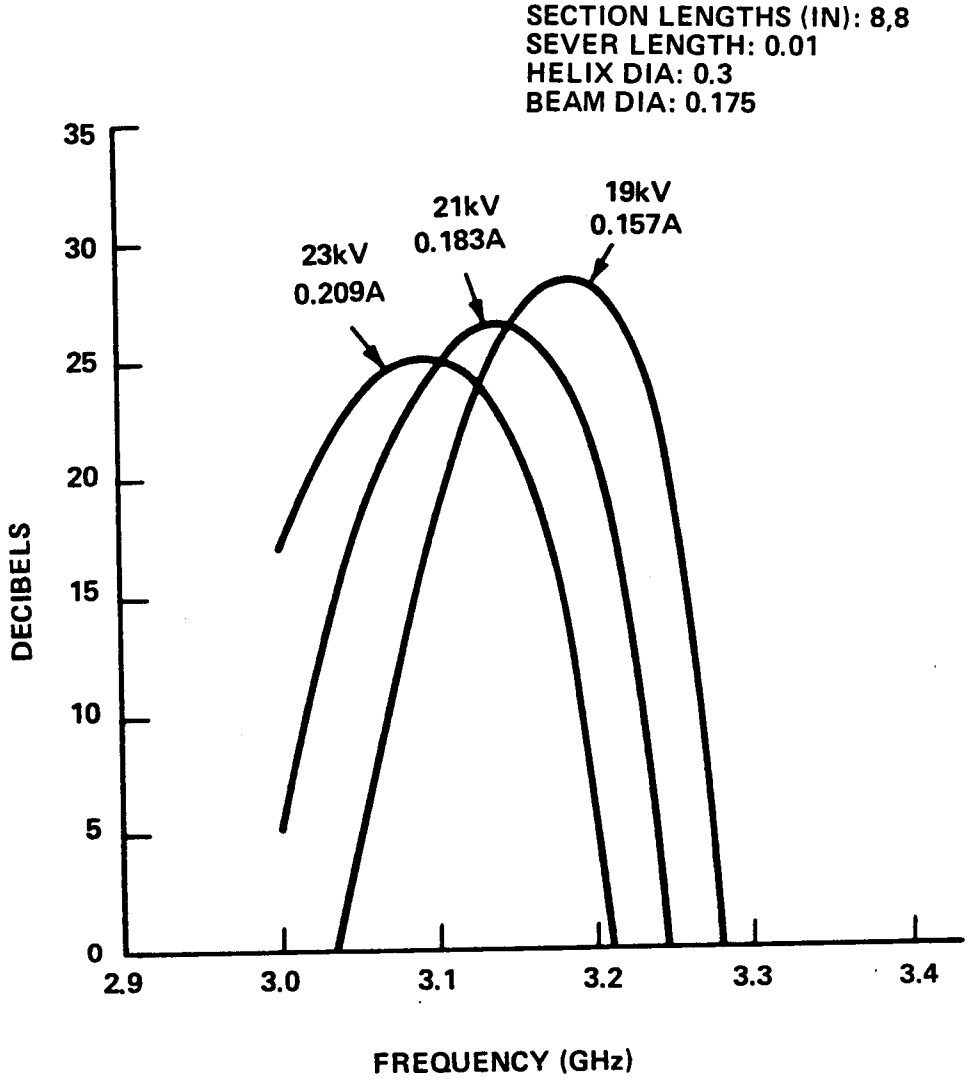

FIGURE 9. SMALL-SIGNAL GAIN VS FREQUENCY (NO LOSS)

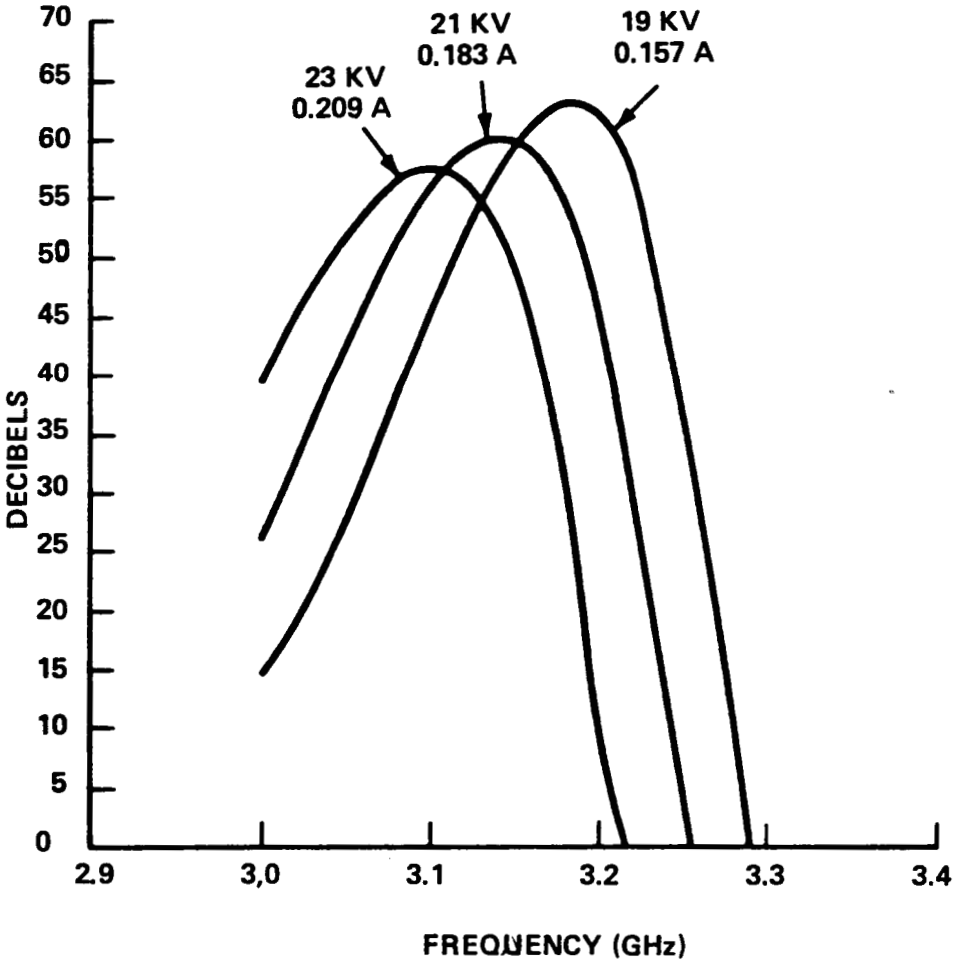

FIGURE 10. SMALL-SIGNAL GAIN VS. FREQUENCY, "Q" = 500

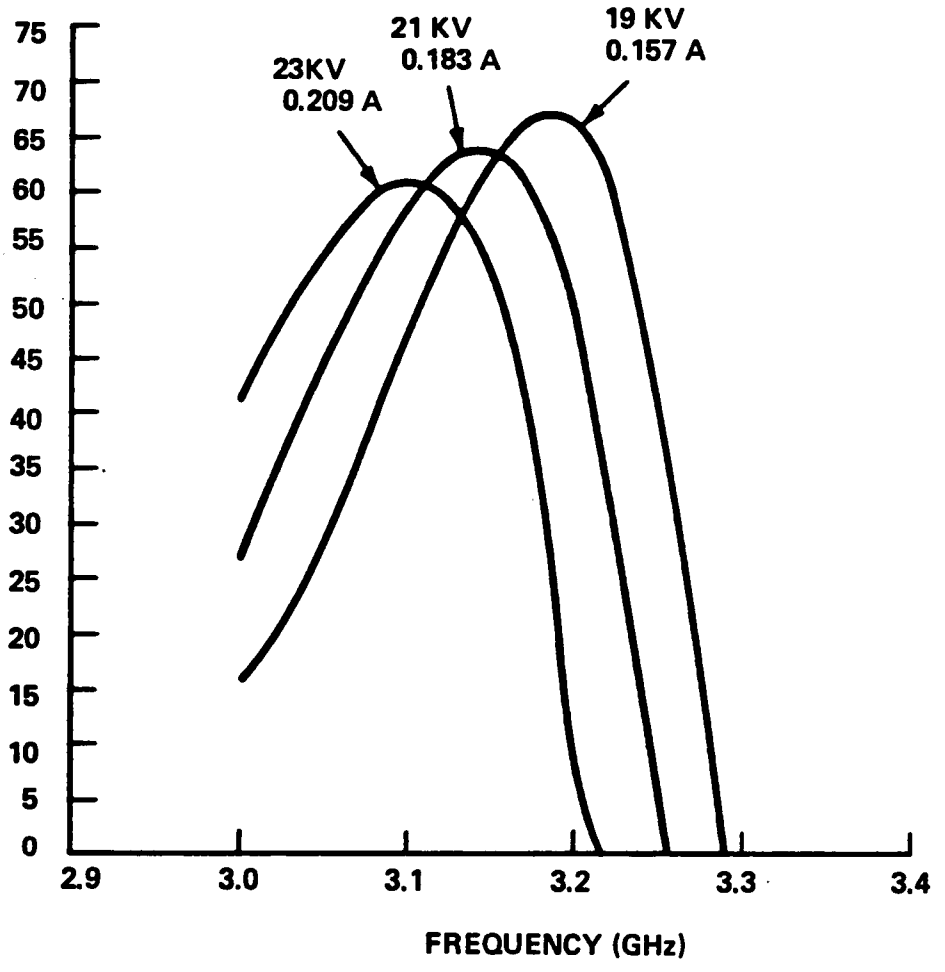

FIGURE 11. SMALL-SIGNAL GAIN VS. FREQUENCY, "Q" = 1000

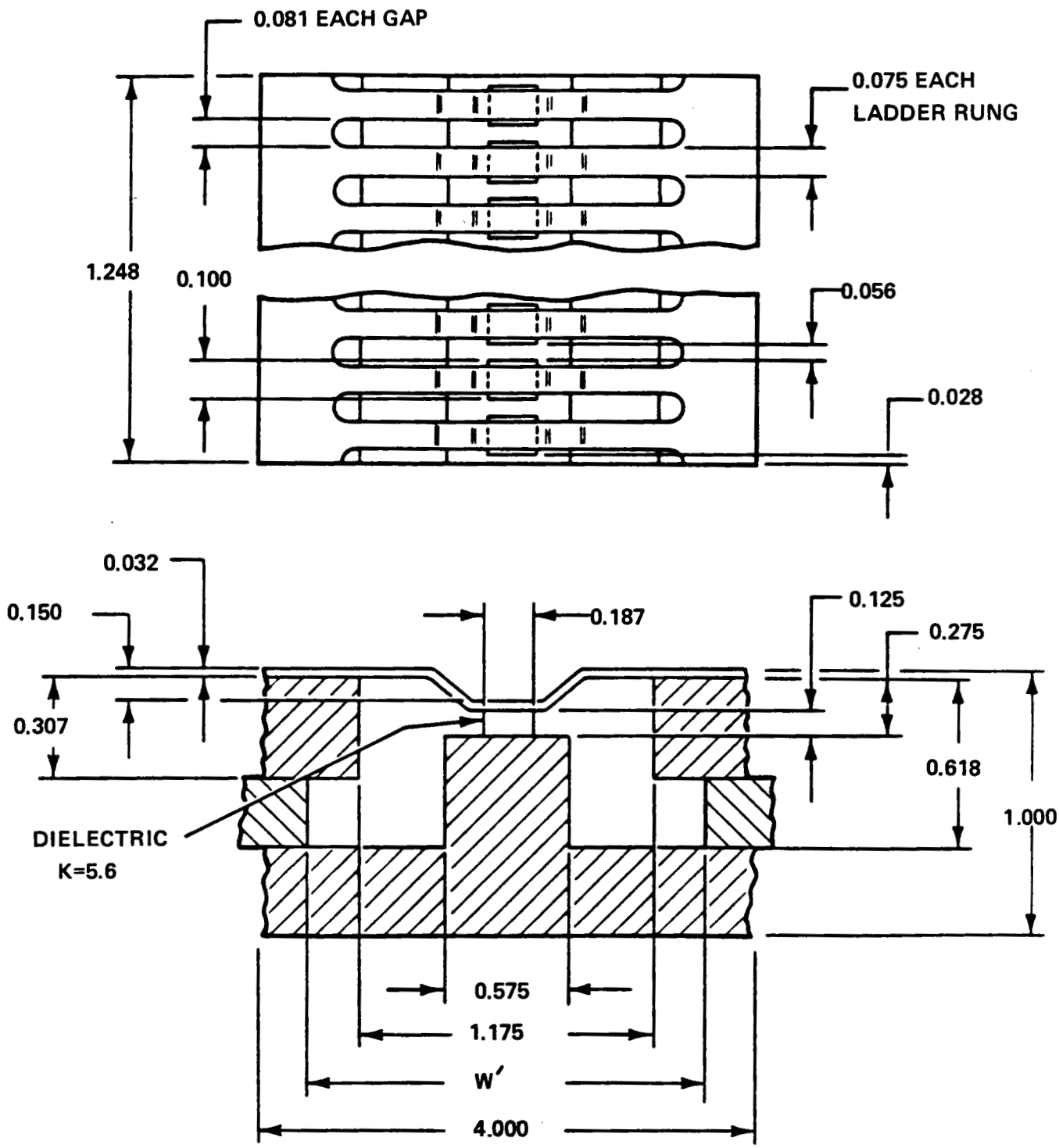

FIGURE 12. HALF OF THE FINAL SCALED COLD-TEST MODEL

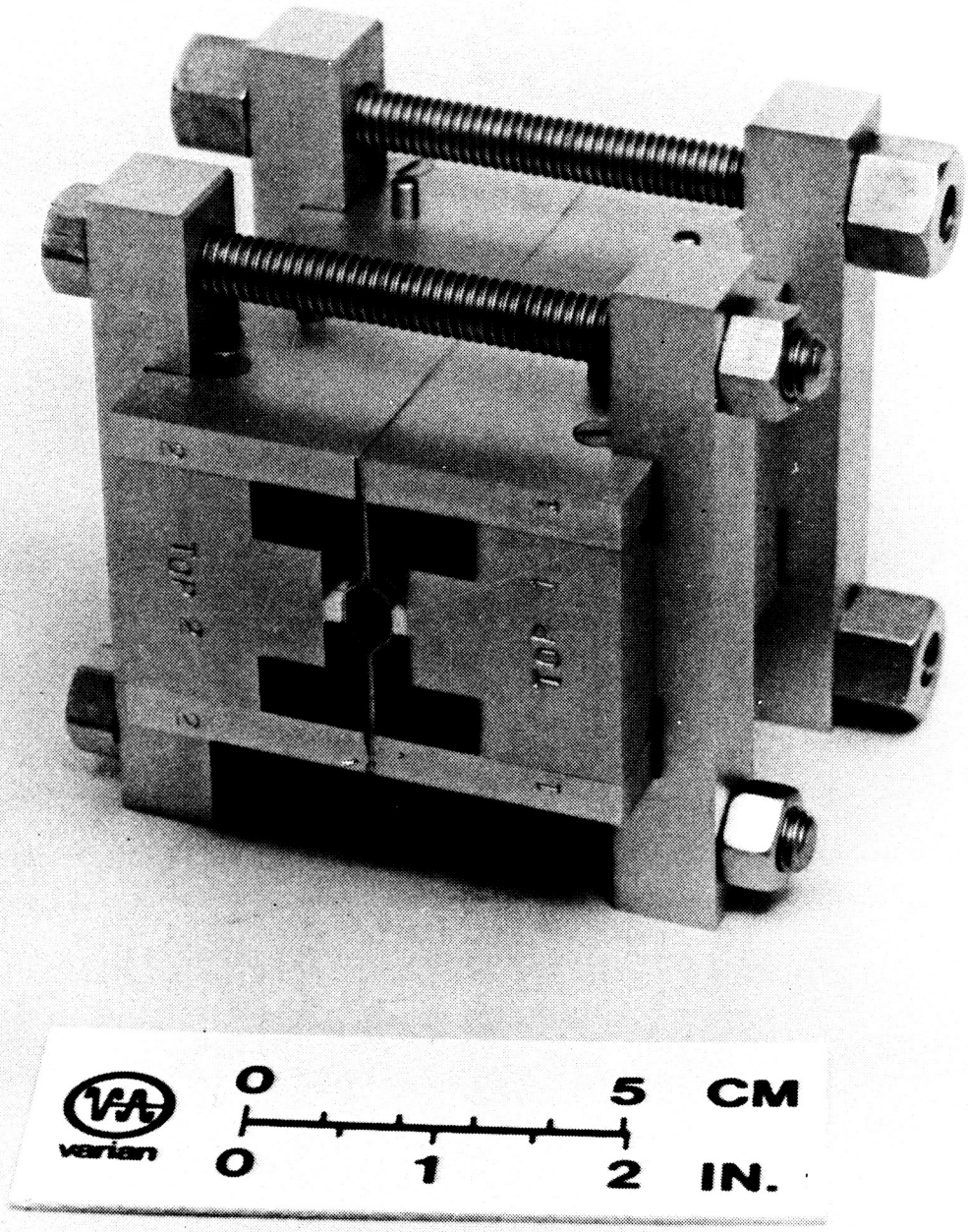

FIGURE 13. 29 GHz / 10 kV TUNNELADDER CIRCUIT GEOMETRY –IN 10X COLD-TEST SCALE MODEL (DIAMONDS SIMULATED BY STYCAST BLOCKS)

F1118

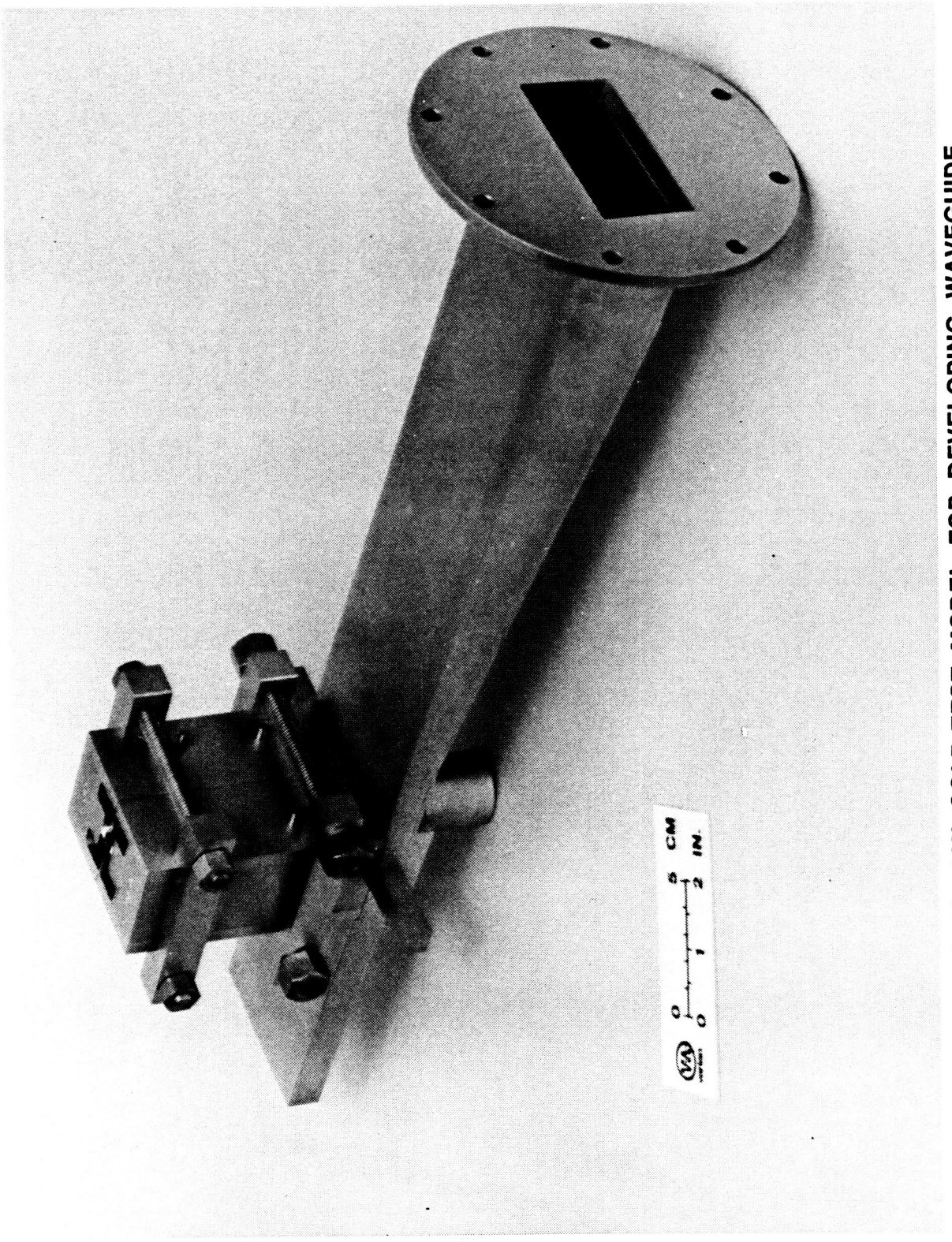

FIGURE 14. 10X COLD-TEST MODEL FOR DEVELOPING WAVEGUIDE TRANSITION

F1118

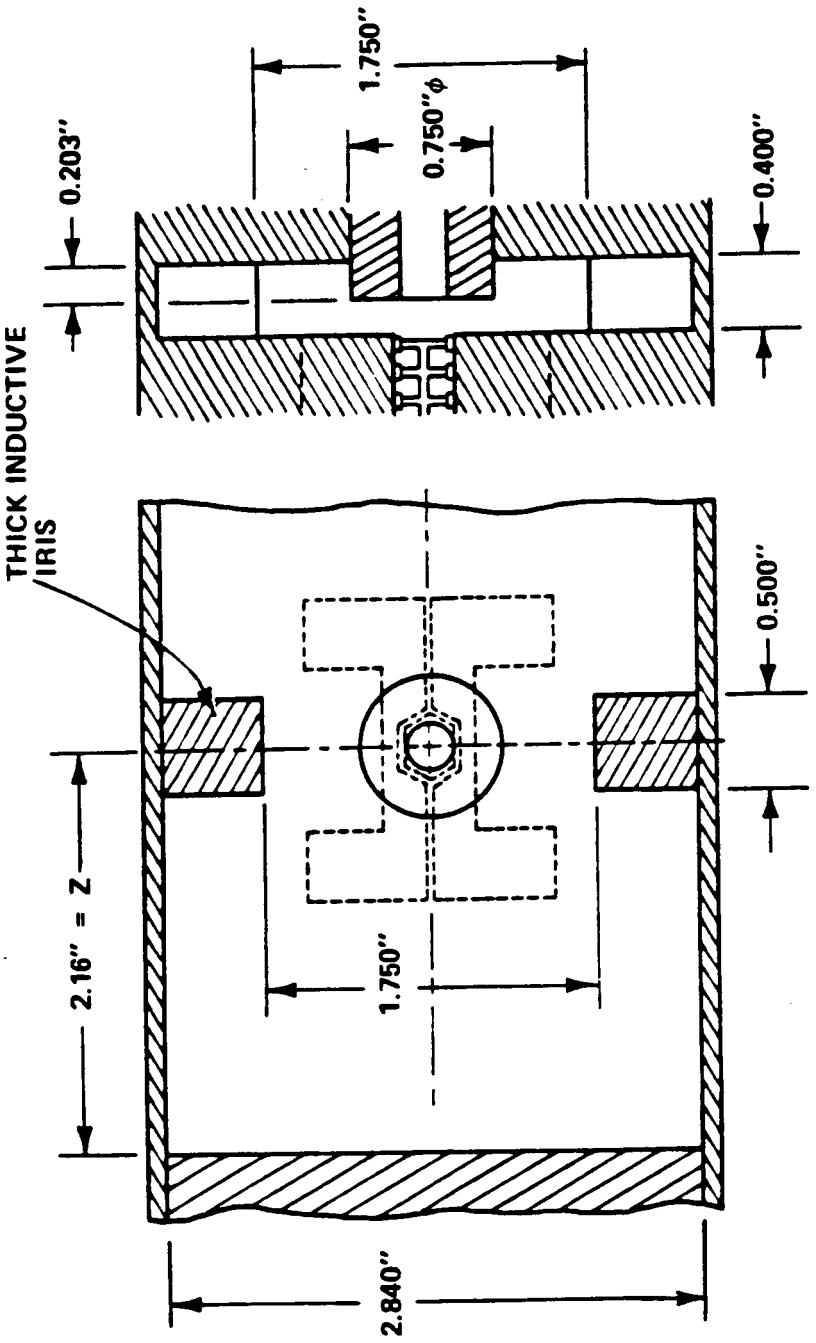

FIGURE 15. CIRCUIT/WAVEGUIDE COUPLER DESIGN (10 X SCALE)

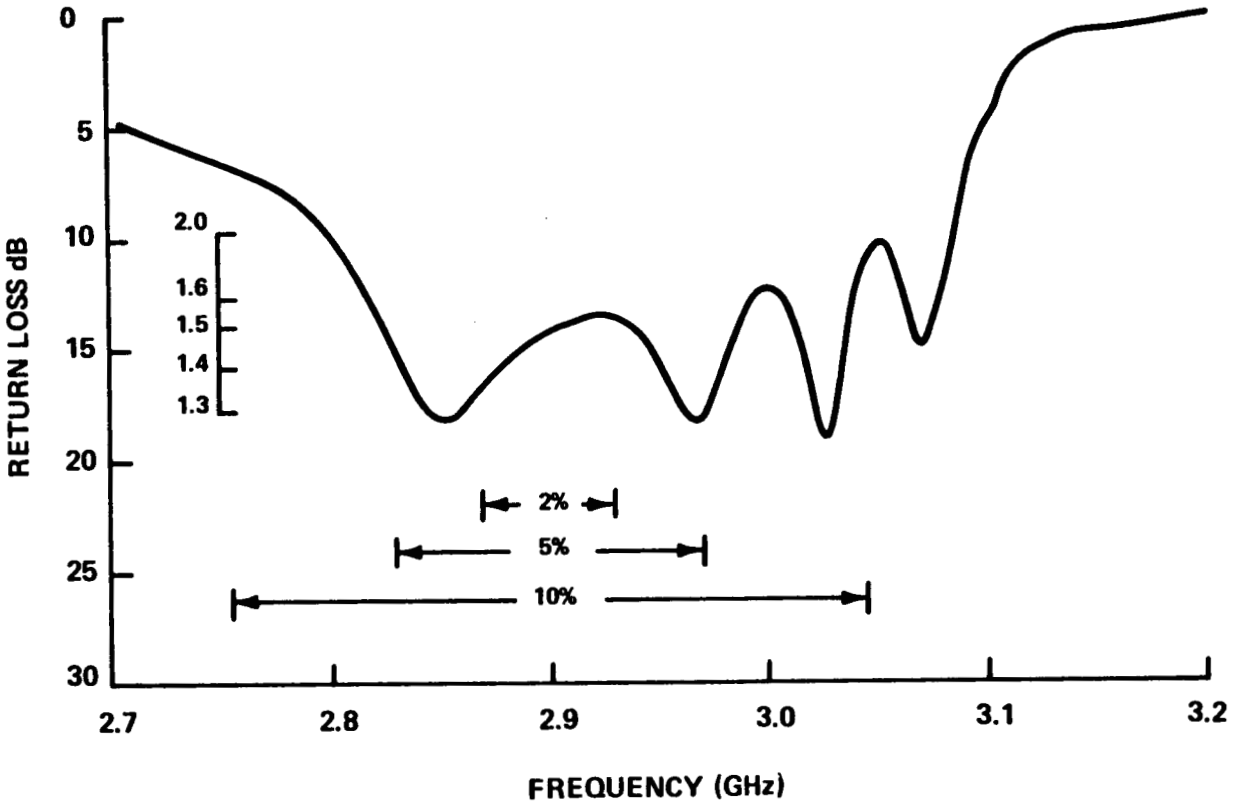

FIGURE 16. COLD-TEST WAVEGUIDE TRANSITION MATCH

3.0 FABRICATION EXPERIMENTS

Fabrication of TunneLadder TWTs has benefited from the investigation of innovative fabricating techniques. Because the circuit has features not often found in other microwave tubes, most of these investigations have been used to solve circuit fabrication problems.

3.1 CIRCUIT BONDING TECHNIQUES

The problems associated with heat dissipation in microwave tubes become acute above 20 GHz. Since most cross-sectional dimensions are inversely proportional to the square of the frequency, energy densities become prohibitively high. In addition, rf losses increase with frequency to the point that only materials with low electrical resistivity can be used in circuit elements. In general, only copper and certain copper alloys are used, thus requiring that circuits be kept at substantially lower temperatures than is necessary at lower frequencies, where refractory metals are more widely used. As stated in Section 2, this combination of circumstances has led to the use of Type IIA diamond as a circuit support material. Both the ridge and the ladder are made of copper. Therefore, a good copper diamond bond is the most important single technique that must be mastered in the successful construction of TunneLadder TWTs.

At the onset of this program, a viable method, composed of a sequence of proven steps, existed for making successful circuit brazes. This method had been developed on earlier TunneLadder programs. It consisted of using chemically milled ladders (see Figure 17) made of a copper alloy (Amzirc) that contains a small percentage (0.15%) of zirconium. The latter element is an active metal, and makes possible direct bonds to the diamond.

The brazing of the ridge Amzirc strip to the OFHC block was resolved by processing as follows:

1. OFHC Ridge — Hydrogen fire at 1000°C.
   — Vac Fire at 1000°C.

2. Amzirc Strip — Chemically clean surface (either Cyanide or Sulfuric Acid).
   — Vac fire at 1000°C.

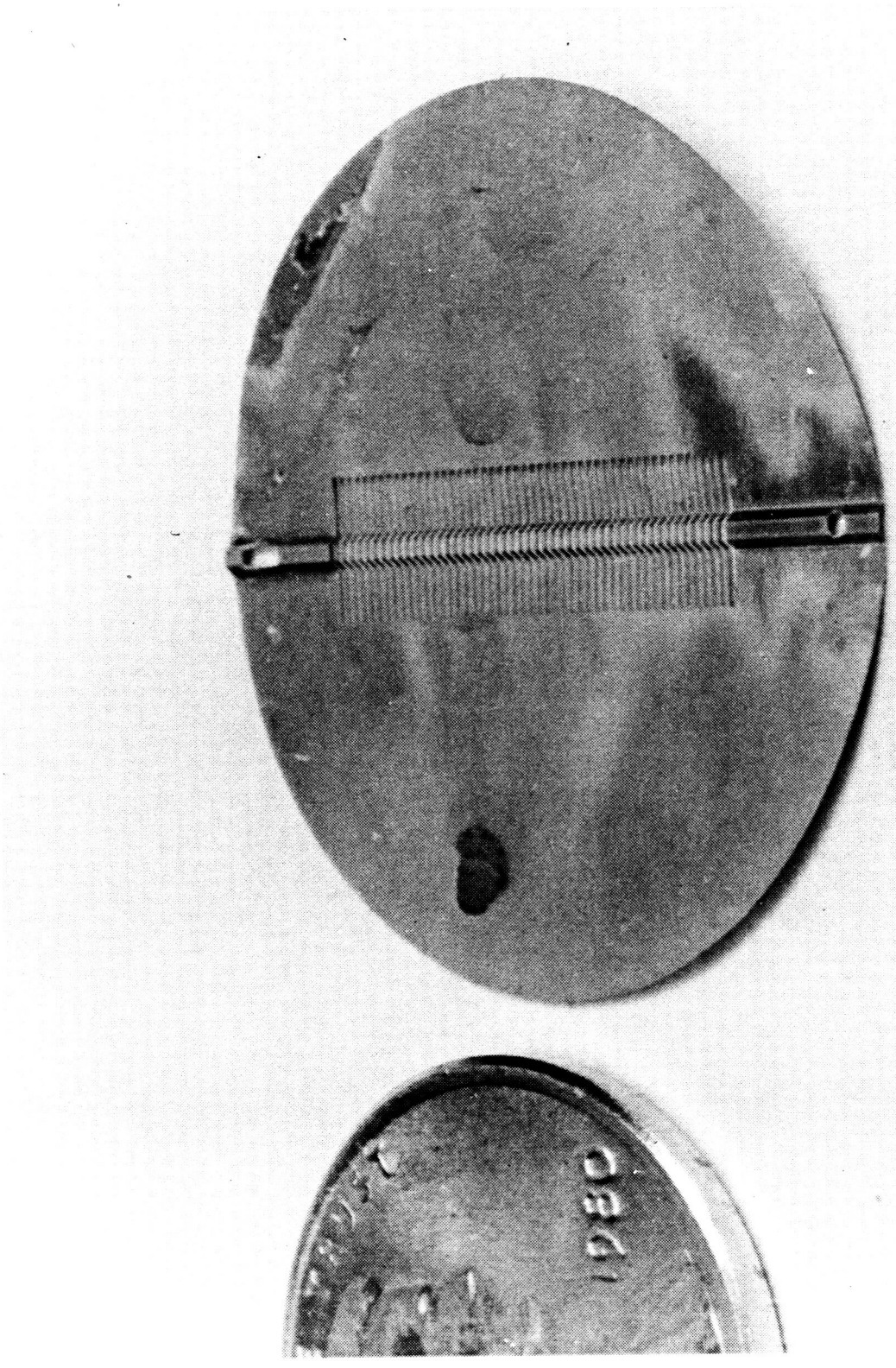

FIGURE 17. CHEMICALLY MILLED, FORMED LADDER ELEMENT OF 2.5 MIL AMZIRC (PITCH – 12.5 MILS)

F1118

3. Braze both in Helium at 1000°C. Braze in a SS 304/Moly fixture that was cleaned by hydrogen and vacuum firing at 1000°C. The fixture keeps a positive pressure between the Amzirc and OFHC ridge block by molybdenum wrap wire around the SS 304 outer parts of the fixture. The brazed assembly was strong and clean.

When diamonds were brazed to the Amzirc strip, two assembly problems were discovered. In the first, removal of the tool steel spacing shims resulted in at least four diamonds moving during the procedure. As a result of this problem, a modification to the procedure was instituted. It consisted of brazing the diamonds to the Amzirc ridge using CRS spacing shims. After the initial braze, the fixture is reworked and other fixtures are used to set the height of the diamonds and to braze the TunneLadder circuit elements.

A second assembly problem was uncovered when a tool steel rail support lifted from the copper ridge block during the brazing of the TunneLadder circuit element to the diamonds, thus separating them. This problem was corrected by eliminating all tool steel fixtures.

Initially, cold-rolled steel was used for the spacing shims, but an etching procedure that produced consistent results could not be established. Therefore, the material was changed to Hastelloy, a nickel-molybdenum-iron alloy. This material proved to be satisfactory in all respects, and was used during the balance of the program.

A number of experiments were performed to determine whether or not a gold diffusion bond was necessary, in addition to the active metal braze, to ensure a good bond between the ladder circuit elements and the diamonds. Both gold sputtering on the circuit elements and gold foil were used as a means for providing the gold needed to create a good diffusion braze. Without the presence of gold, good contacts were not consistently made, even with contact pressures high enough to distort the cross-sectional configuration of the circuit element. One possible method for overcoming the problem of low contact pressure without distorting the circuit element is to make the circuit element out of dispersion-strengthened copper. Such a material is Glidcop, a form of OFHC copper with Al_2O_3 powder dispersed through it. The active metal, zirconium, would then be sputtered onto the Glidcop parts. At one point in the program, Glidcop circuit elements were ordered, but they were not used as the gold diffusion bond method, while cumbersome, proved to be quite reliable. In addition, there is some evidence that Glidcop will swell and distort when in the presence of molten braze material. Methods for eliminating this problem include sintering the copper circuit element to the copper body without

using braze material, and sealing over the alumina "pores" with sputtered or plated copper a few microns thick. However, these avenues were not investigated.

A final change in the brazing technique was the use of stainless steel as a material for pressing the diamonds down during the firing that bonds them to the waveguide ridge. Initially, the hold-down element had been made from tungsten, as it is not subject to distortion under combinations of high temperature and pressure. However, when brazing with a tungsten fixture, the diamonds at the end of the row would not maintain good contact with the ridge. This phenomenon led to the conclusion that the tungsten fixture, whose expansion coefficient is substantially lower than that of copper, caused shear forces to develop at the copper/diamond interface. When the tungsten fixture was replaced by a stainless steel fixture, this problem was eliminated.

In summary, the circuit fabrication experiments led to the following observations and conclusions concerning copper/diamond bonds:

1. An active metal must be present; the zirconium content of Amzirc provides this.

2. The brazing atmosphere must be totally contaminant-free, lest very weak bonds result. Helium is used as it has fewer contaminants than are typically encountered in "vacuum brazing".

3. The brazing temperature must be as low as possible to further minimize contamination risk; 800°C has been selected.

4. All fixtures must be designed to avoid creating shear forces in the copper/diamond interface plane which would provoke bond failure. Chemically milled copper fixtures are therefore used for spacing, and Type 304 stainless steel fixtures (expansion coefficient same as for copper to within 1%) for applying pressure to the diamond dice. (Although tungsten, with its ability to resist deformation under pressure, might be preferable, its thermal expansion coefficient is only about 24% that of copper, whereby the contraction difference on cool-down could break the diamond/copper bonds.)

5. Rung/diamond bonding must not cause ladder rung distortion. Given the small rung cross section (see above), the pressure needed for true active metal

bonding would indeed result in distortion. The technique is therefore supplemented by gold-diffusion bonding, which is also used to attach the ladder-rung ends to the enclosing cavity.

3.2 CIRCUIT ELEMENT FABRICATION

As indicated in the introduction, the TunneLadder is a potentially inexpensive alternative to the conventional, coupled-cavity slow-wave structure for high average power, millimeter-wave applications. In the TunneLadder, a large number of superbly machined cavity and drift tube parts are replaced by a single pair of ladder elements. These ladders were manufactured by Elcon, Inc. of San Jose, California. A photograph of the ladders used on this program is shown in Figure 17. The process that Elcon uses allows the raw material to be formed in its nonplanar configuration prior to photoetching. In addition, the photomask which serves as a master for the etching process can be made at 20 times actual scale. Under these circumstances, the tolerances on individual rung and gap dimensions can be held to within ± 0.0002 inch. Likewise, the overall length can be controlled with equal accuracy, thereby eliminating the problem of tolerance accumulation which inevitably occurs when many parts are used. Additionally, because all of the parts are made from a single master, repeatability will be much more certain than it is for the equivalent machined parts.

Plans were made to have some parts made by electronic discharge machining (EDM), as this process is typically less expensive than photoetching. However, since the quantities to be used were limited and the photoetched parts were quite satisfactory, the order was not placed.

3.3 BODY ASSEMBLY TECHNIQUES

Other techniques, while not entirely foreign to TWT design, bear mentioning as unusual process applications. For example, at the interface between the waveguides and the circuit blocks, good contact and RFI shielding is provided by gold plating the mating surface on the waveguide assembly. Use of this process in the place of a furnace braze greatly simplifies the assembly procedure.

The use of machine screws inside the vacuum envelope represents another means for reducing fabrication complexity. The screws were made of the same 300-series stainless steel

as is used for other internal tube parts, so no contamination problems are introduced. Also, all screws used in blind holes are drilled on axis, to prevent virtual leaks.

Heliarcing is also used more extensively than in other TWTs. All of the cooling tube assemblies are made to be Heliarced, and all of the major subassemblies, except the collector, are installed in the final assembly with Heliarc welds.

4.0 TUBE DESIGN

4.1 GUN DESIGN

The cold test and computer results indicate that the optimum operating voltage for the circuit, as built, is 21 kV. Some initial gun calculations were made under the assumption that the tube might also operate successfully at 17 kV and 133 mA. Under those circumstances, a tube with a 0.014-inch-diameter beam and an average cathode loading of 2 A/cm^2 would require a gun design with an area convergence of only 67. While such a design would have a large margin for good focusing performance, the efficiency estimates for 200 W CW rf power are very optimistic.

Therefore, a more cautious approach was taken. This decision led to projections of a tube operating at 21 kV and 183 mA. A gun used in a high voltage application (50 kV) had all of the necessary properties for use in our configuration, if scaled. This gun had a cathode cylindrical radius of 0.375 inch, and produced a beam with an 0.0356 inch diameter, as demonstrated on a beam analyzer, giving an area convergence ratio of 110.

Scaling this gun by a factor of 2.54 would produce a 0.014-inch-diameter beam and a gun with a cathode cylindrical diameter of 0.147 inch, giving a cathode loading of 1.6 A/cm^2.

The gun structure with the 0.375-inch-cylindrical diameter has a built-in isolated anode capable of being operated at very high voltages, thus allowing tube operating perveances (i.e., as related to cathode voltage and beam current) equal to or less than the basic gun perveance. In this case, the basic gun perveance is 0.258 μ perveance and tests could be made at 0.06 μ perveance, which is the tube operating perveance for the present design. For 0.06 μ perveance the mod anode was run at 4.6 kV above a cathode potential of -12 kV (w.r.t. ground). When tested in a beam analyzer, the 0.375-inch-diameter gun initially produced a beam with a ripple of 9%, but by changing the cathode voltage to -20 kV, and adjusting the anode voltage accordingly, the ripple was reduced to 1.5%.

Before a 0.147-inch-diameter gun assembly was built, a gun assembly with a 0.165-inch-diameter was found with the same geometry and support structure as the 0.37-inch-diameter gun assembly. This gun produces a beam with a 0.0157-inch-beam diameter, which would be satisfactory if the ripple was low. As indicated in the previous paragraph, the ripple is exceptionally low, so that the 0.165-inch-diameter gun can be used with confidence. The cathode loading for this gun is 1.3 A/cm^2.

Finally, a 0.165-inch-diameter gun assembly was tested using a short section of 0.025-inch-ID body as a tube structure. Tests covered a voltage range from 21 kV to 42 kV and a perveance range of 0.05 to 0.09 μ perveance. The magnetic focusing field covered a range from 75% to 125% of 2.5 times Brillouin. The transmission was better than 98% in all cases and in all but one was better than 99%. Since the above assembly design exists and performs so well, no additional design changes were made.

4.2 FOCUSING STRUCTURE DESIGN

Initial magnetic focusing structure design work was based on the gun information described above. The final magnet and pole piece design was also based on the results of tests done on the beam stick described in Section 4.2.1. The magnetic structure design is subject to the following constraints:

1. If possible, the gun and collector pole pieces should conform to existing designs for these assemblies.

2. For the sake of ease of tube assembly, two radially focused ring magnets will be used.

3. Magnet material will be commensurate with the present state-of-the-art in rare-earth/cobalt materials, which is a samarium cobalt magnet with an energy product of 22×10^6 gauss-oersteds.

4. The magnet gap must allow sufficient space for the circuit and related assemblies. Given the estimated gain/length of 27.9 dB/in., a desired small-signal gain of 30 dB, and allowing for an anode assembly and a tail pipe assembly to protect the circuit, the gap must be at least 2.5 inches long.

Given all of these constraints, a computer analysis of the first cut was made. The geometry of this initial approach is shown in Figure 18, with the field plots, flux density, and flux lines shown in Figures 19, 20, and 21 respectively. The magnitude of the magnetic field in the gap is satisfactory, but the field in the cathode region has to be shaped, and the field in the collector region has to be reduced to as low a value as possible. These goals were

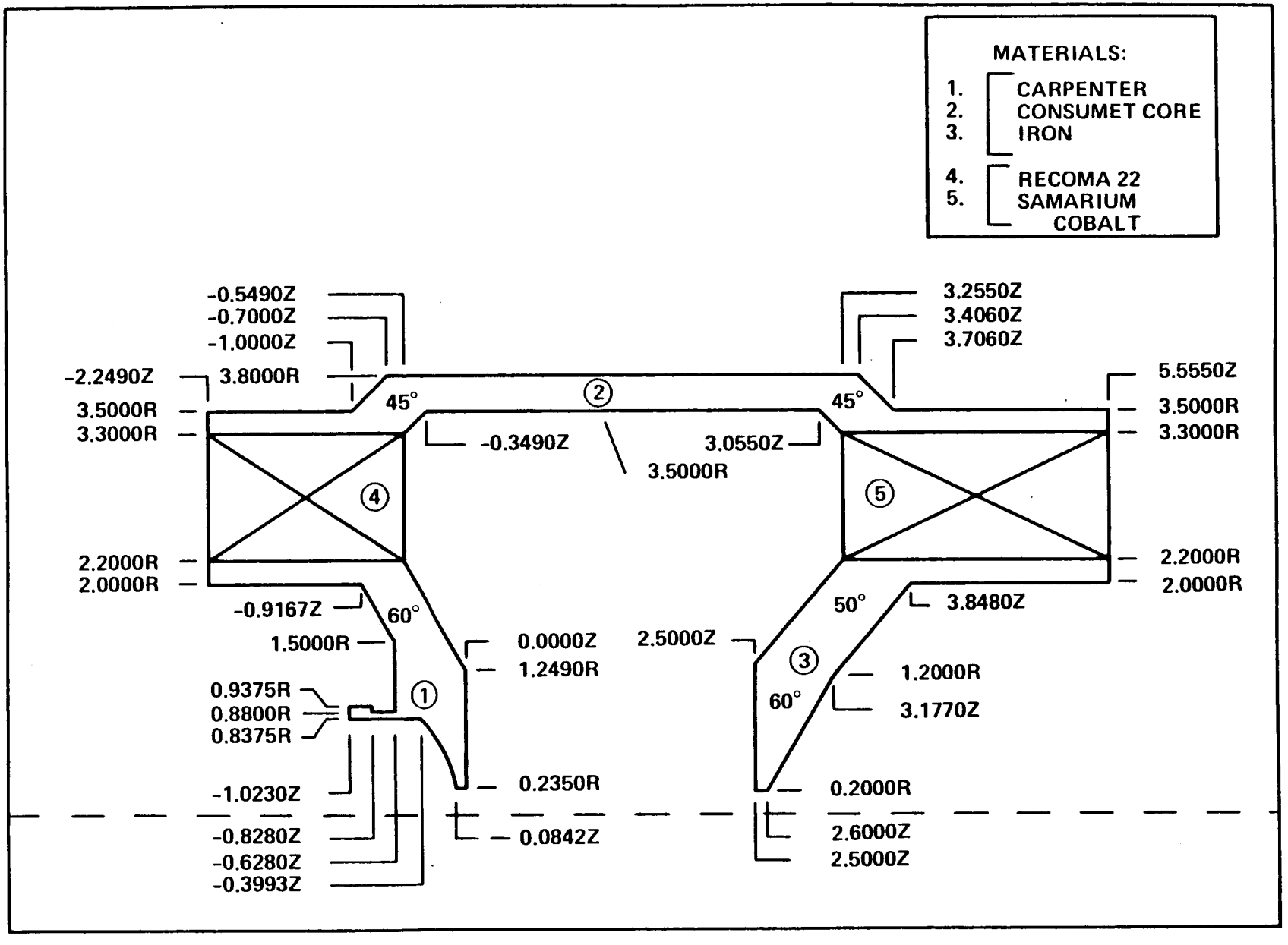

FIGURE 18. VTQ-6299A1 DESIGN 1: MAGNET CIRCUIT

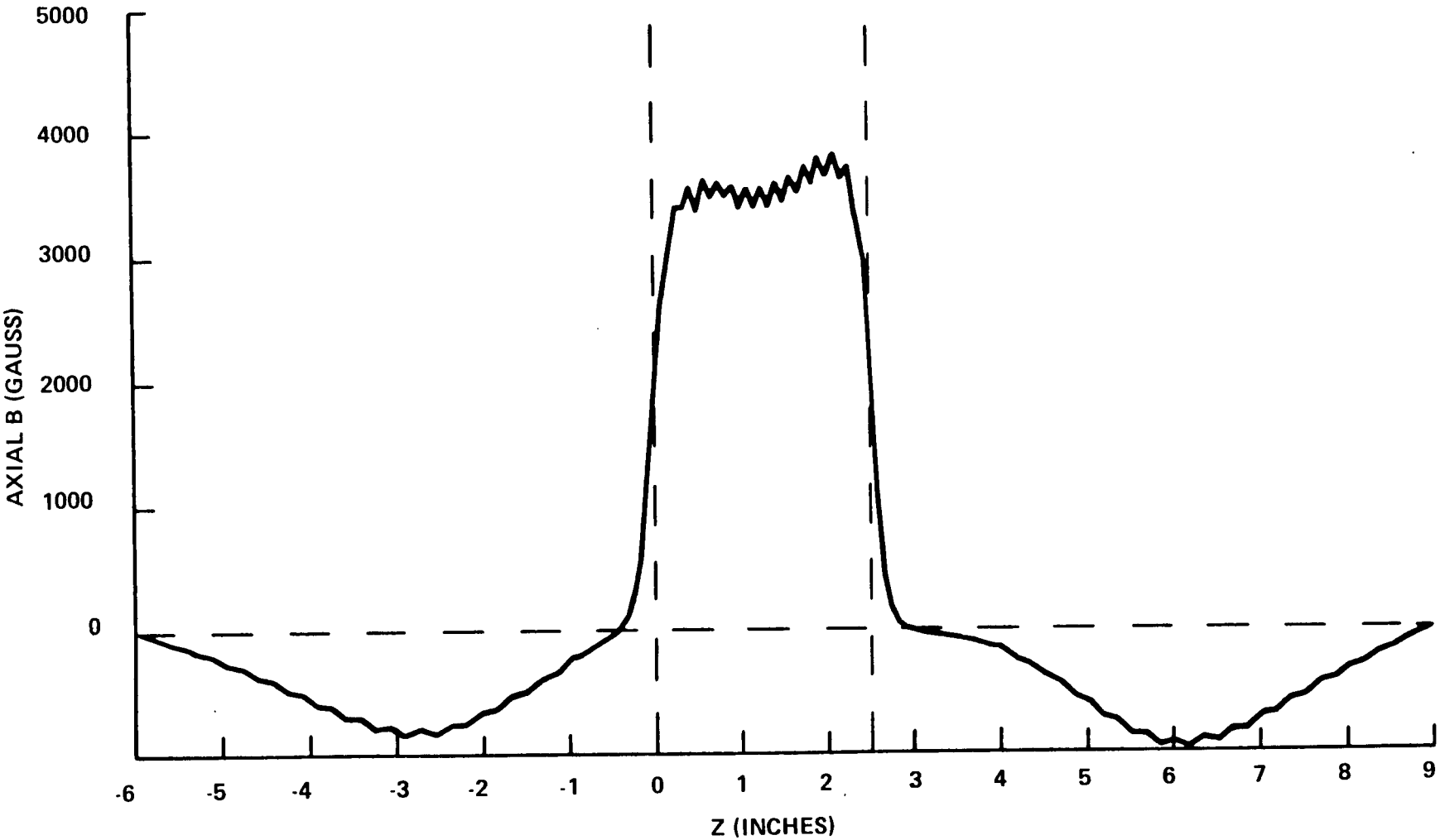

FIGURE 19. VTQ 6299A1 DESIGN 1: AXIAL B FIELD

F2637
F1118

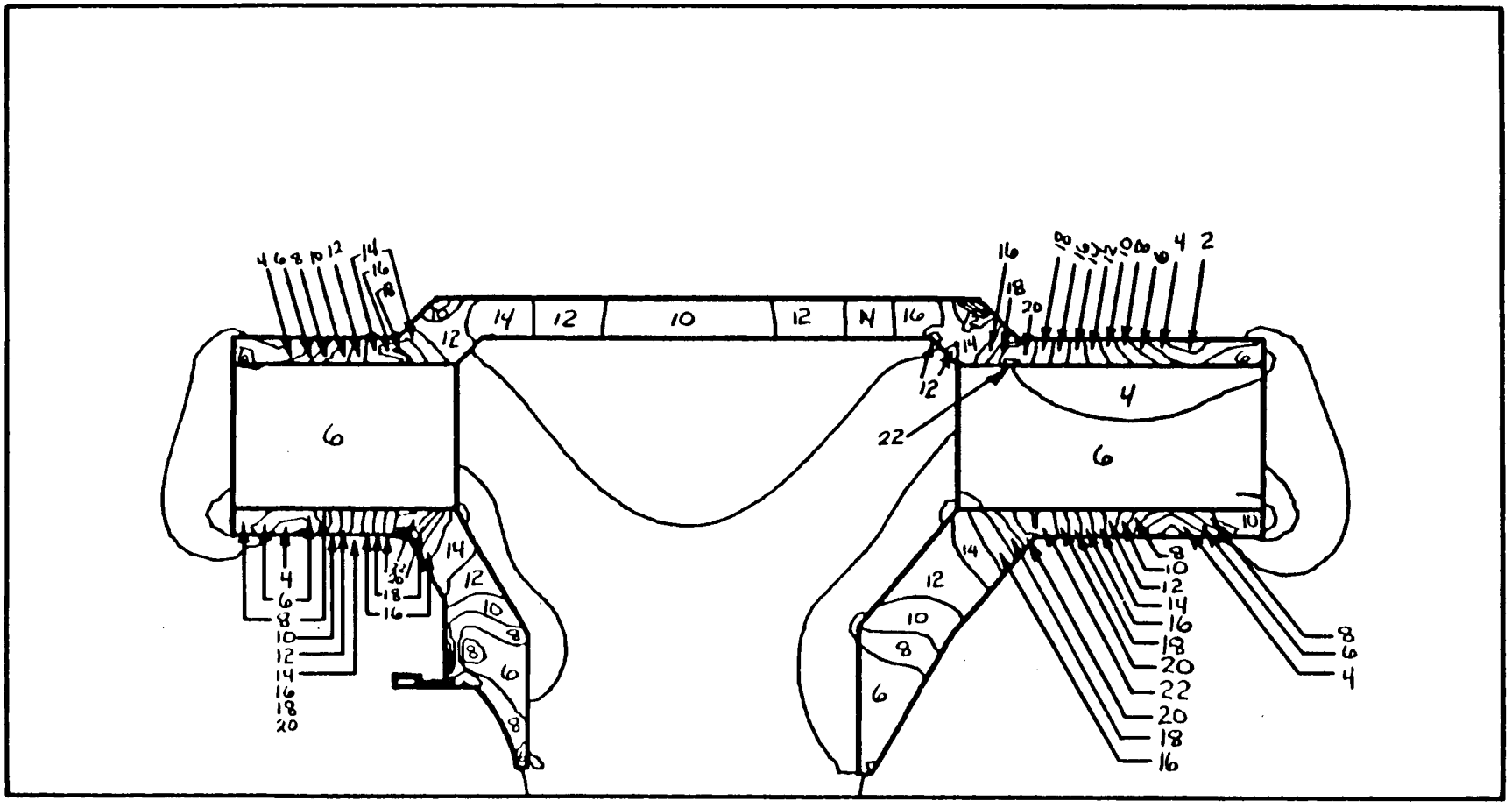

FIGURE 20. VTQ-6299A1 DESIGN 1: MAGNITUDE OF B IN IRON (K GAUSS)

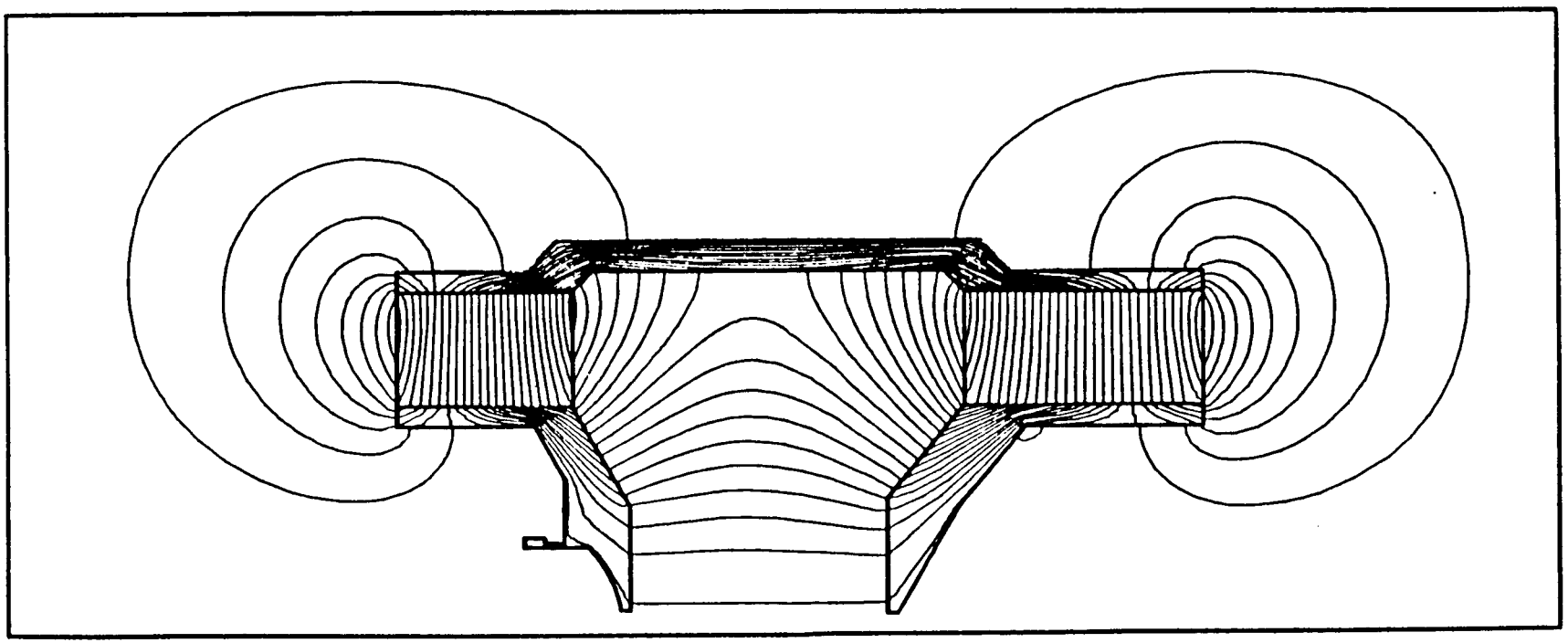

FIGURE 21. VTQ-6299A1 DESIGN 1: FLUX LINES

accomplished in both designs 4 and 6, whose gap fields are nominally 2.5 times Brillouin and 2.0 times Brillouin respectively.

At this point, the beam stick described below was tested, after which the decision was made to use the 2.0 times Brillouin design. A final design was analyzed which included minor changes necessary to provide easier mechanical assembly. The field plots for designs 4 and 6 are shown in Figures 22 and 23, and the entire analysis of design 7 is shown in Figures 24, 25, 26 and 27. This assembly is 9.2 inches in diameter and 9.0 inches high.

4.2.1 Beam Stick

In order to verify both cathode and focusing structure designs, a device was designed, built and tested with the same overall configuration as a tube, but in which the circuit is replaced by a circular drift tube with a diameter equal to the shortest distance across the TunneLadder beam hole. A layout of this device is shown in Figure 28.

Although the actual tube pole piece configuration is used, a solenoid is used in place of the permanent magnets. Under these circumstances, it was possible to vary the axial magnetic field in the beam stick. A set of such field plots is shown in Figure 29. With this information in hand, along with body current measurements from the beam stick tests, the determination was made to use the lower (2.0 times Brillouin) magnetic field design, as indicated above. This design calls for a focusing structure weighing 63 pounds as compared to 84 pounds for the structure that would be required to produce the 2.5 times Brillouin field.)

4.3 CIRCUIT DESIGN

The circuit design used in this program must provide high interaction impedance, at millimeter-wave frequencies, in a geometry that provides for tight, noncumulative tolerances, thermal ruggedness, and straightforward fabrication techniques. The high interaction impedance is necessary to ensure high enough gain per unit length to yield sufficient over-all gain in the allowable length, and high enough beam efficiency to provide sufficient rf output power at the available beam voltage and current. The TunneLadder approach provides such a circuit.

The history of the TunneLadder circuit is described in Section 1.2, the cold testing that yields optimum dimensions is described in Section 2, and the circuit fabrication techniques are

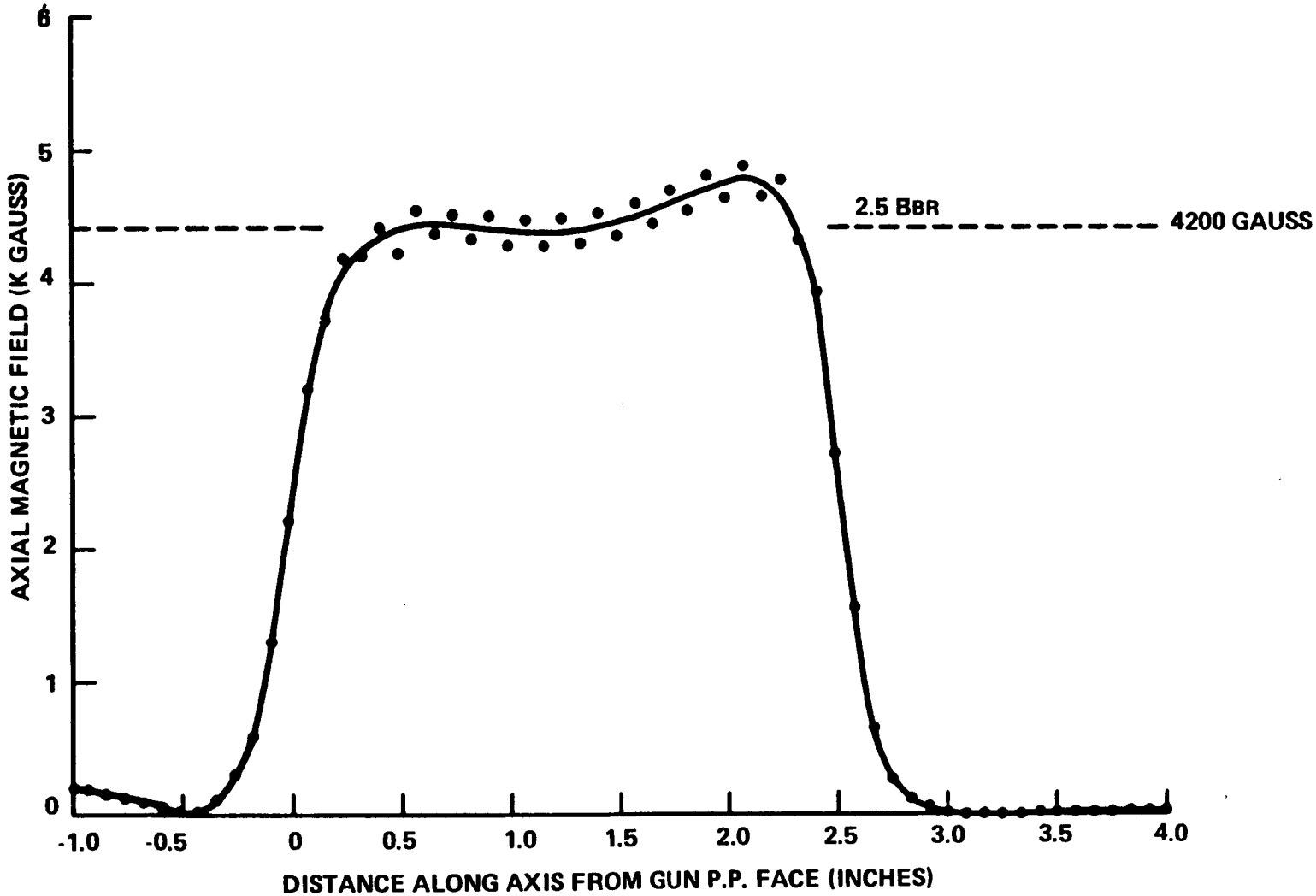

FIGURE 22. VTQ-6299A1 DESIGN 4: AXIAL B FIELD

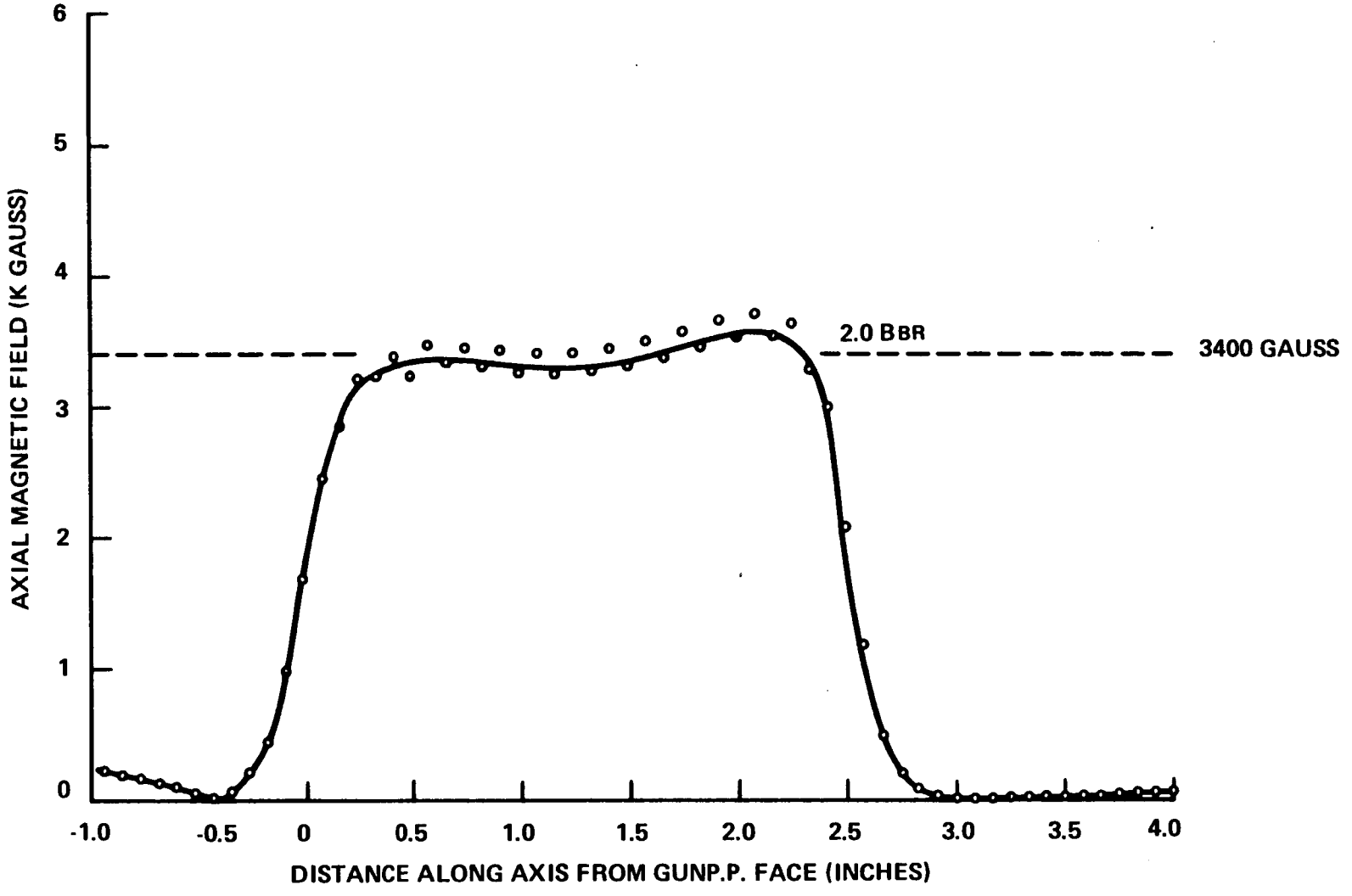

FIGURE 23. VTQ-6299A1 DESIGN 6: AXIAL B FIELD

D2641.
F1118

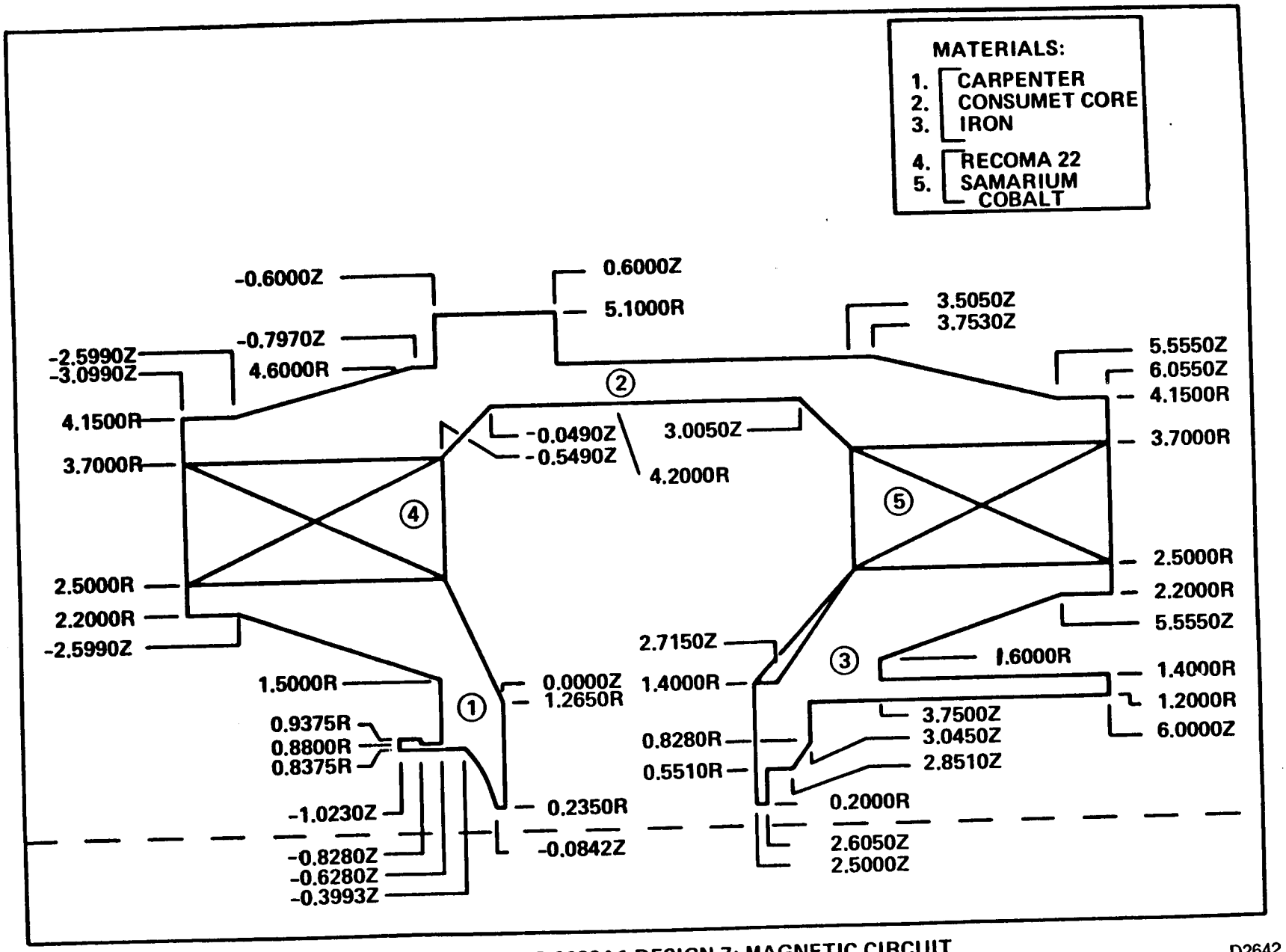

FIGURE 24. VTQ-6299A1 DESIGN 7: MAGNETIC CIRCUIT

D2642
F1118

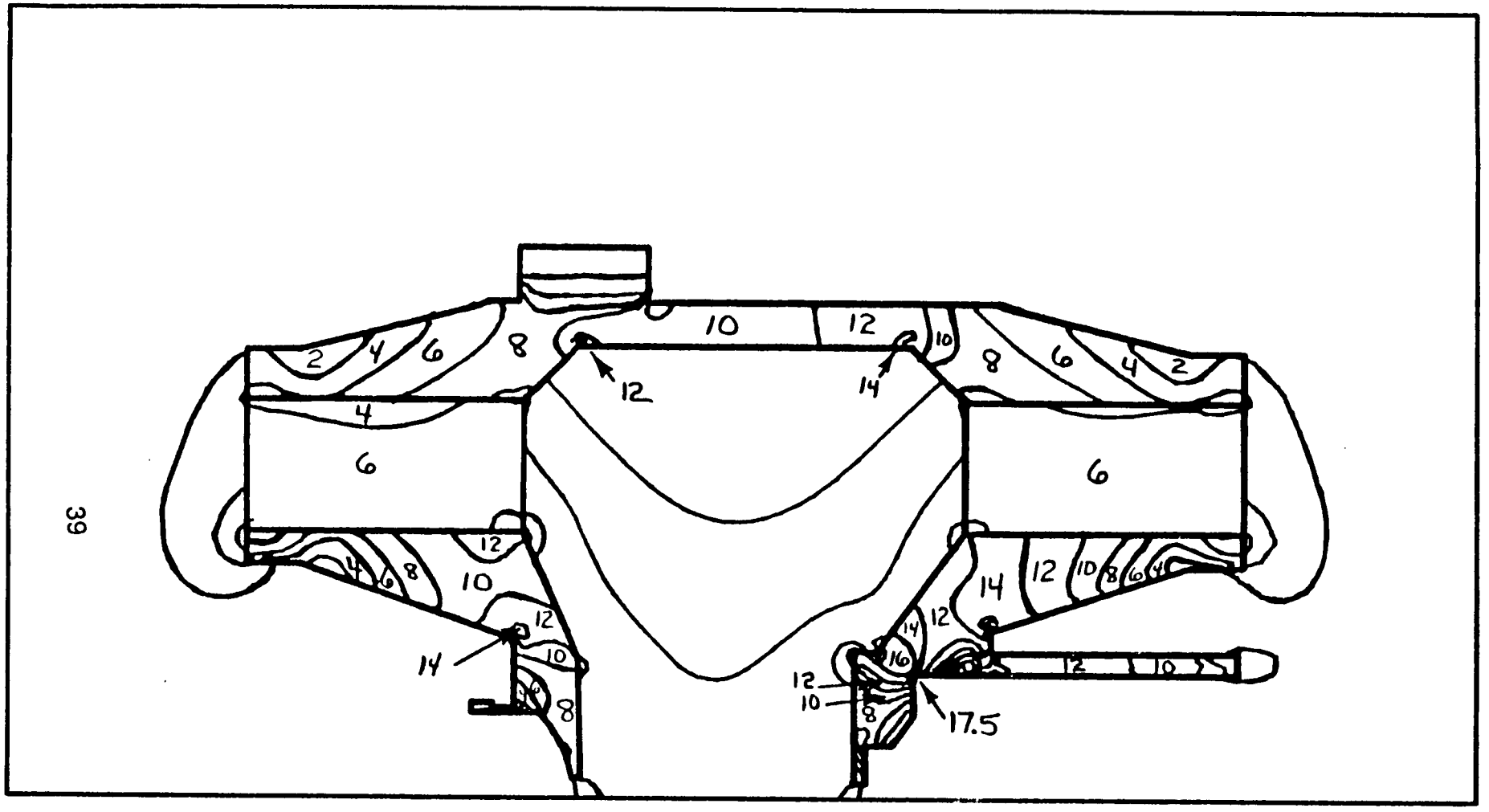

FIGURE 25. VTQ-6299A1 DESIGN 7: MAGNITUDE OF B IN IRON (K GAUSS)

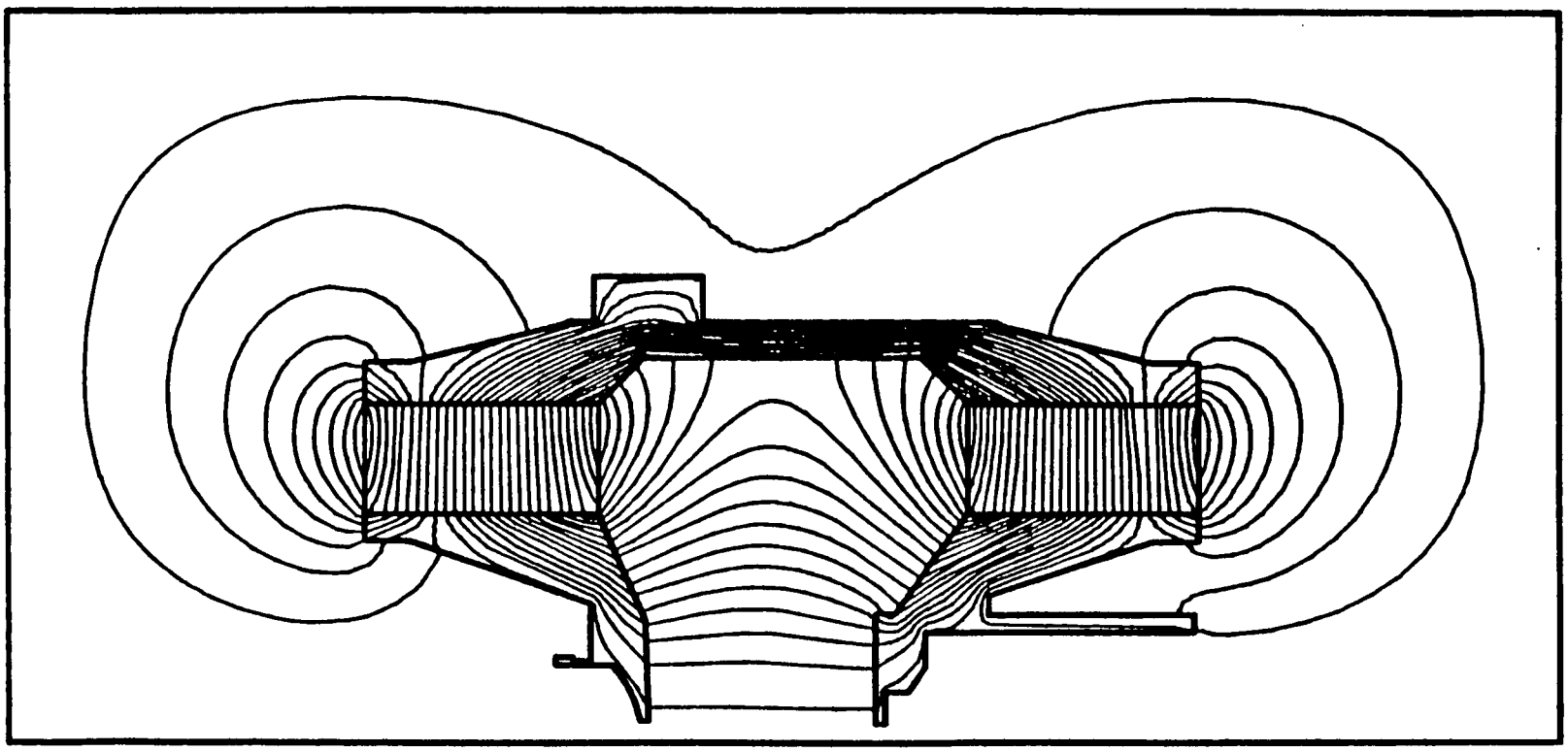

FIGURE 26. VTQ-6209A1 DESIGN 7: FLUX LINES

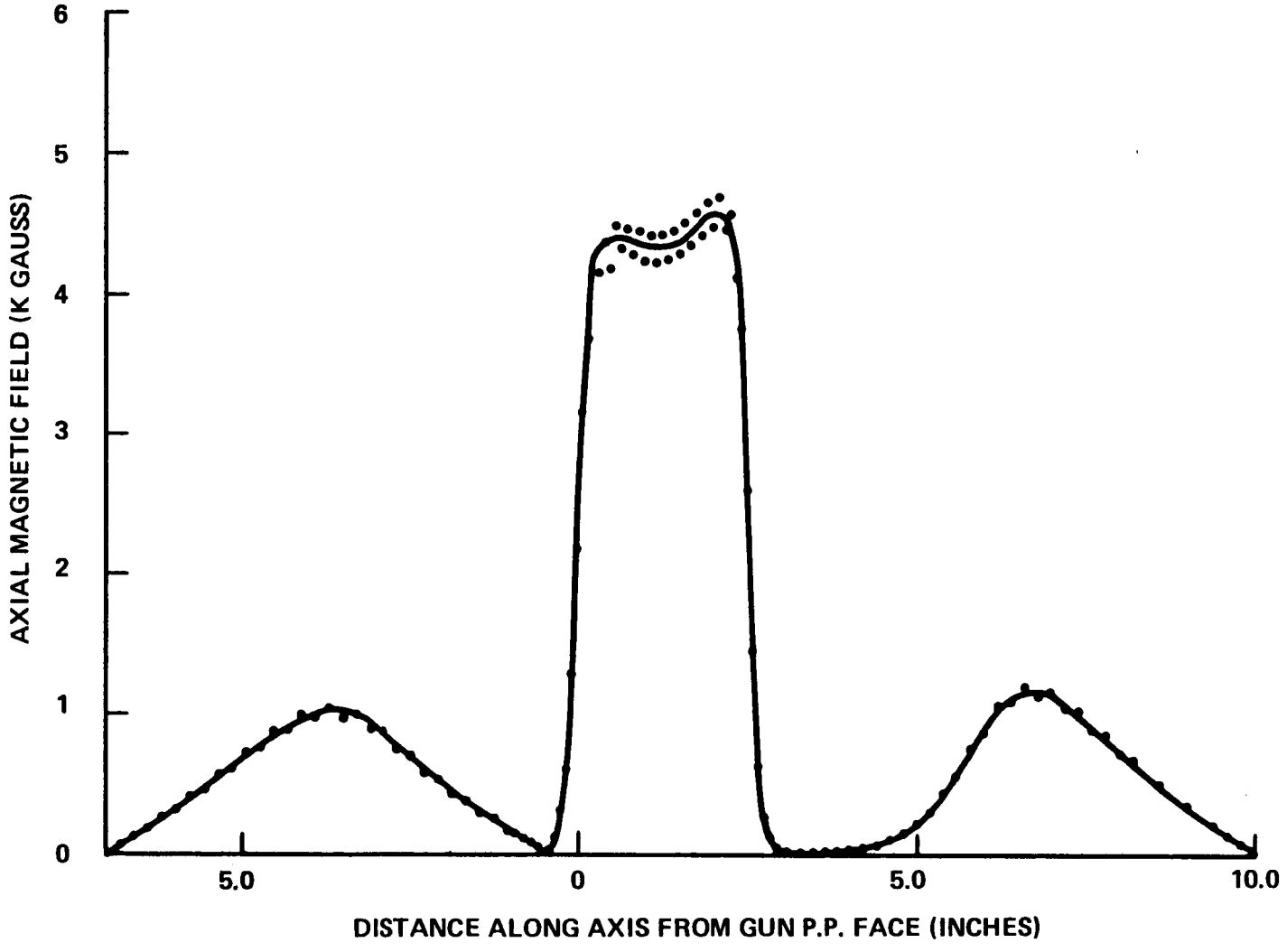

FIGURE 27. VTQ-6299A1 DESIGN 7: AXIAL B FIELD

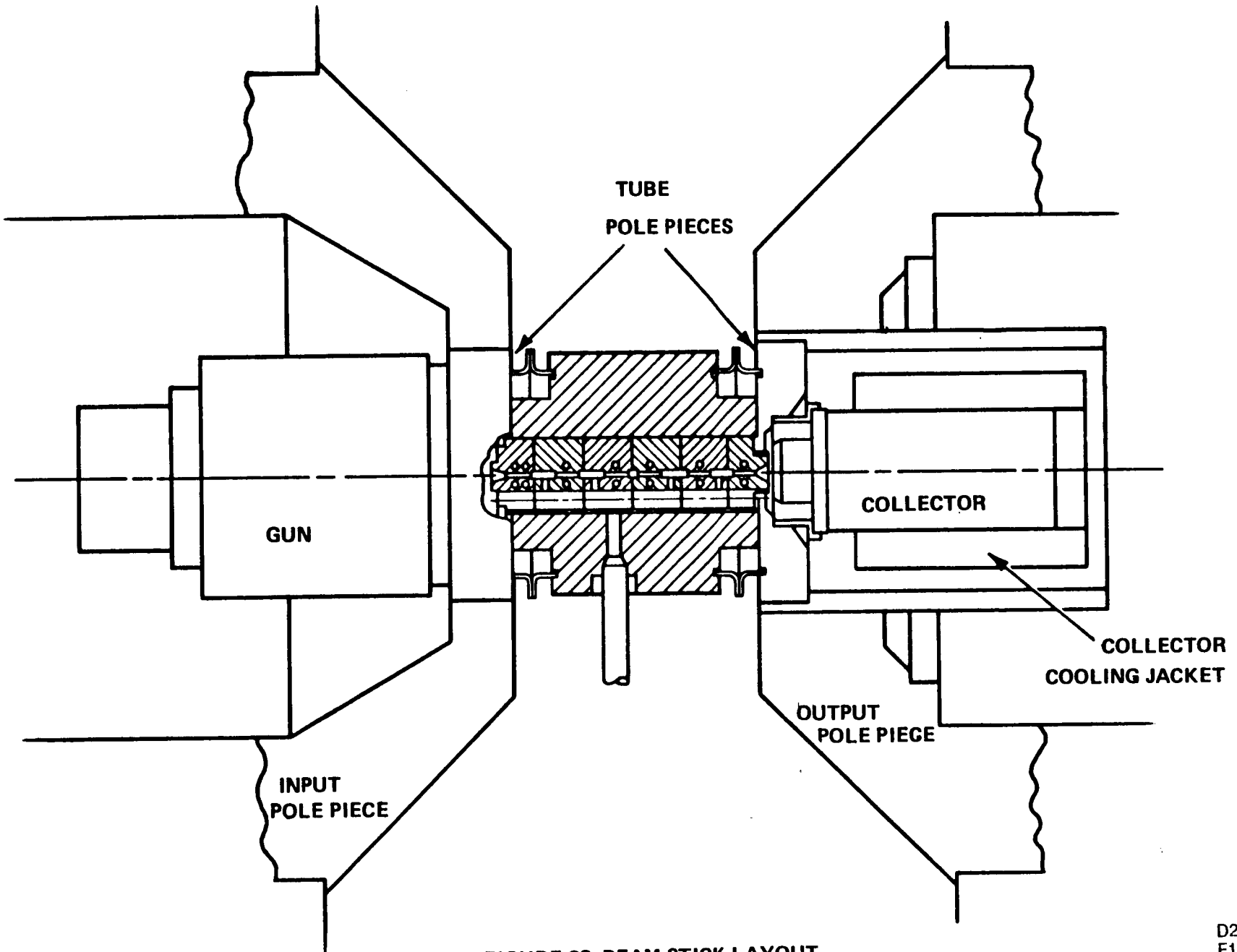

FIGURE 28. BEAM STICK LAYOUT

D2646
F1118

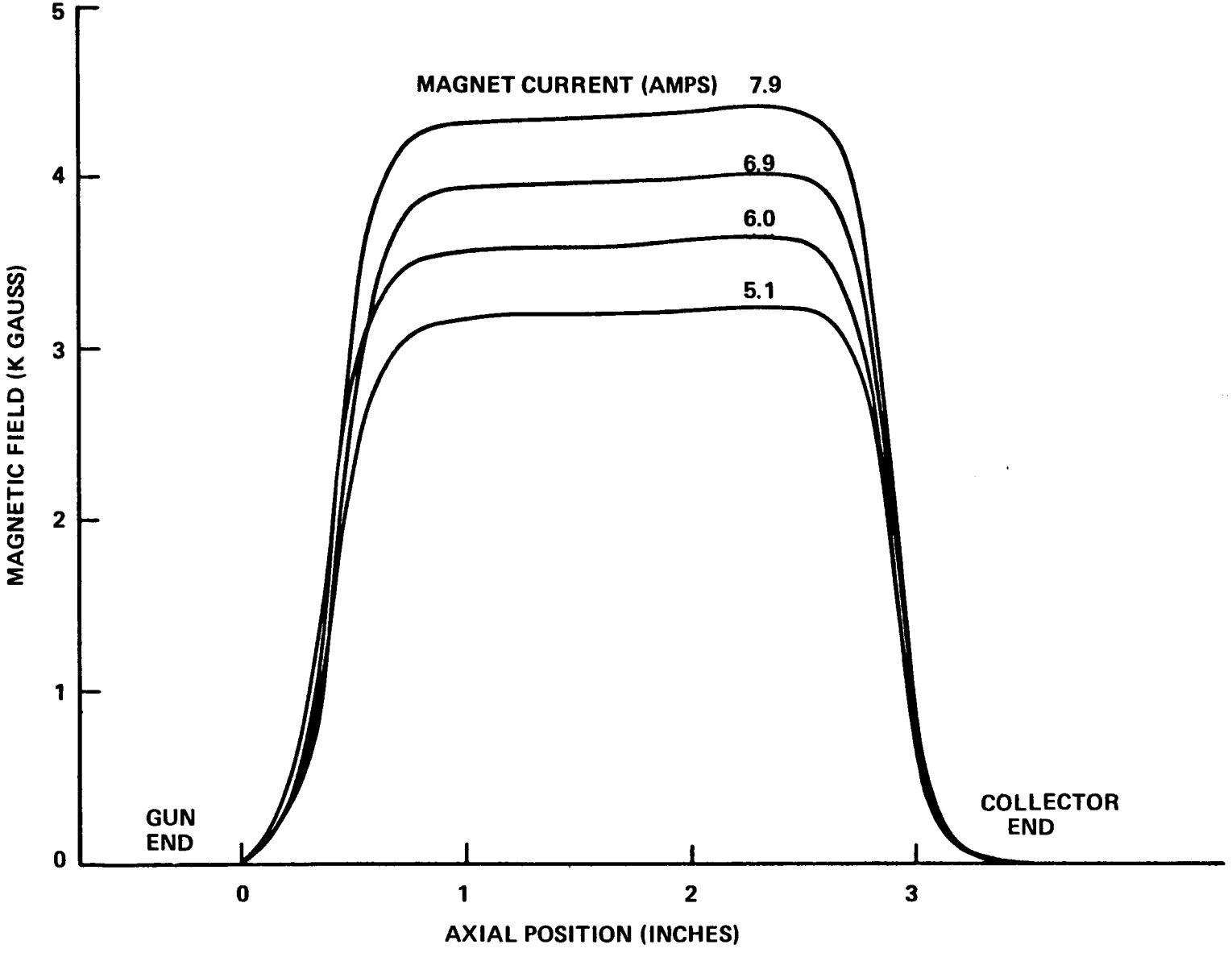

FIGURE 29. ELECTROMAGNET AXIAL FIELD PLOTS

D2647
F1118

given in Sections 3.1 and 3.2. A cross section of the TunneLadder structure, given actual dimensions, is shown in Figure 30. As indicated in Section 2.1, the computed gain per unit length for this circuit is 28.6 dBm/in.

For 25 dB saturated gain, 5 dB compression, and 15 dB launching and sever losses, the total circuit gain must be 45 dB, giving an active circuit length of 1.57 inches. This length has been allocated 0.575 inch to the input section and 1.000 inch to the output. The total length of the circuit assemblies, including 0.120 inch for each of the four waveguide matching elements, is then 2.055 inches.

Once the appropriate materials, techniques, and dimensions had been ascertained, the fixtures were designed which allowed straightforward and reliable assembly. The circuit brazing details, including the appropriate fixtures, are shown in Figures 31 through 35.

Figure 31 shows the brazing of an Amzirc shim to the waveguide block and the subsequent machining to produce the capped ridge. Figure 31 also shows the diamond-to-ridge braze. A detail inset shows the braze fixture, the chemically milled diamond cube spacer and an additional strip of Amzirc foil (to ensure sufficient zirconium atoms at the interface). These are heated in helium at 800°C in the special temperature-compensated fixture. The last inset in Figure 31 shows the metalizing of the top of the diamond cubes. This is achieved with a gold-topped strip of Amzirc foil and special temperature-compensated fixture.

Figure 32 first shows the trimming and height-sizing operation required to prepare the diamond/ridge assembly for brazing to the ladder element. With the graphite fixture shown, the ladder-to-diamond braze is done also at 800°C in helium.

The special temperature-compensated brazing fixture is shown in Figure 33. It uses molybdenum and stainless steel parts which produce a positive pressure on the braze joint during the temperature rise and resultant expansion difference. The fixture has been highly successful; ten assemblies were brazed without any rejects due to loose diamonds (42 diamonds per braze) or weak ladder-rung brazes.

Figure 34 details the procedure for brazing diamond cubes to the ridge block. The machined ridge block, the spacer, and the fixtures are all designed to provide the necessary alignment and pressure.

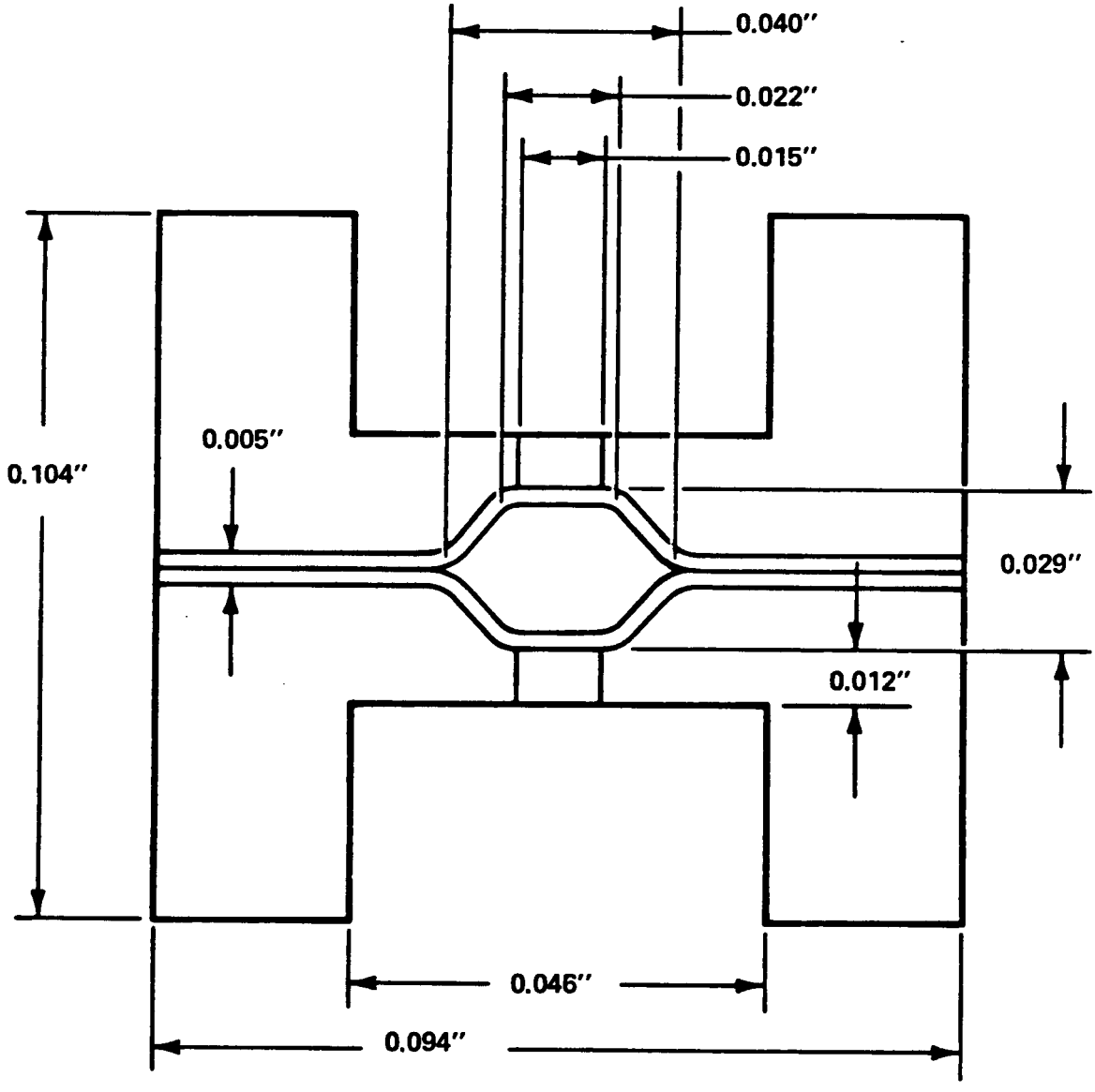

FIGURE 30. CROSS SECTION OF TUNNELADDER INTERACTION STRUCTURE

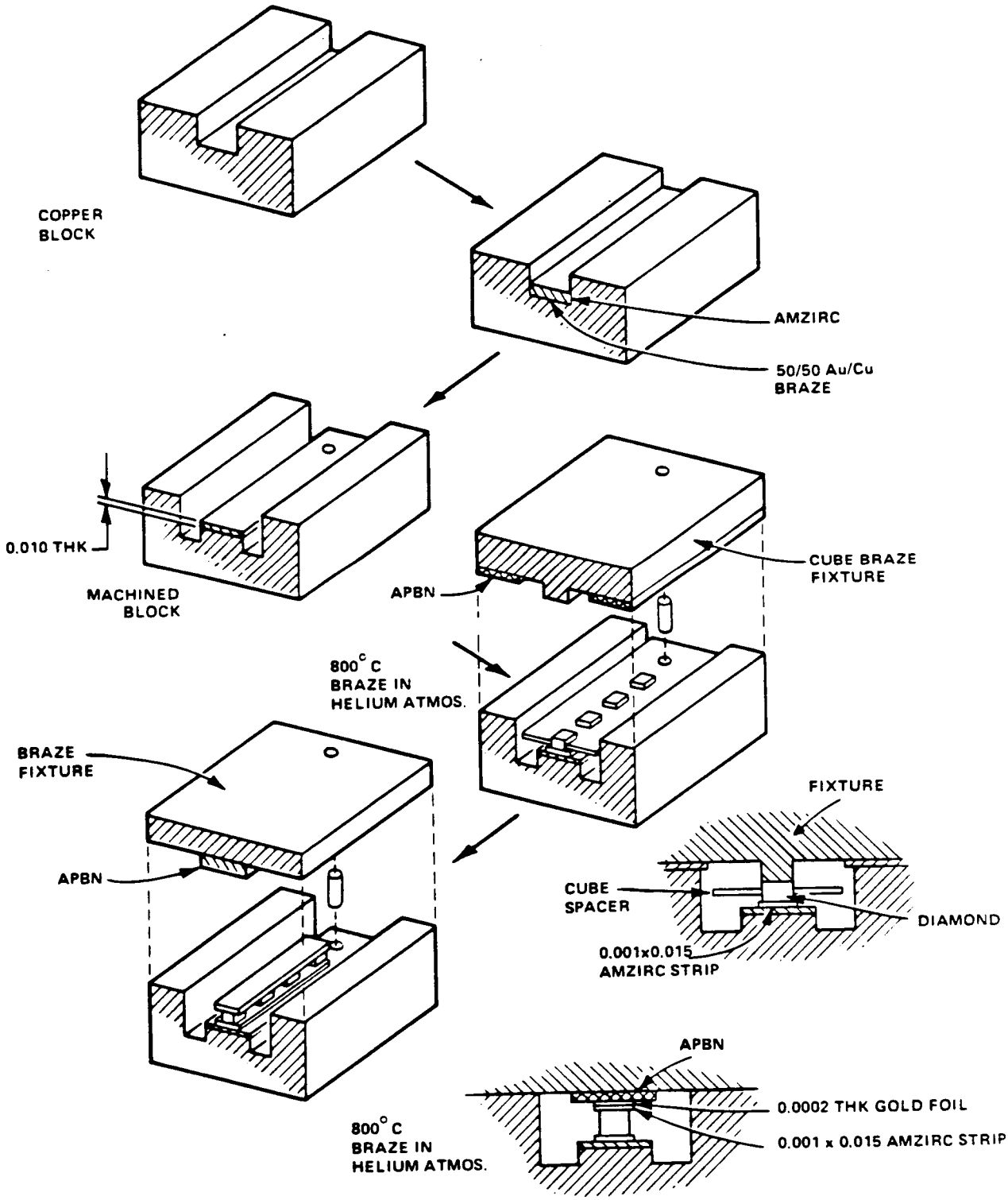

FIGURE 31. ASSEMBLY PROCEDURE THROUGH METALIZATION OF DIAMOND CUBES

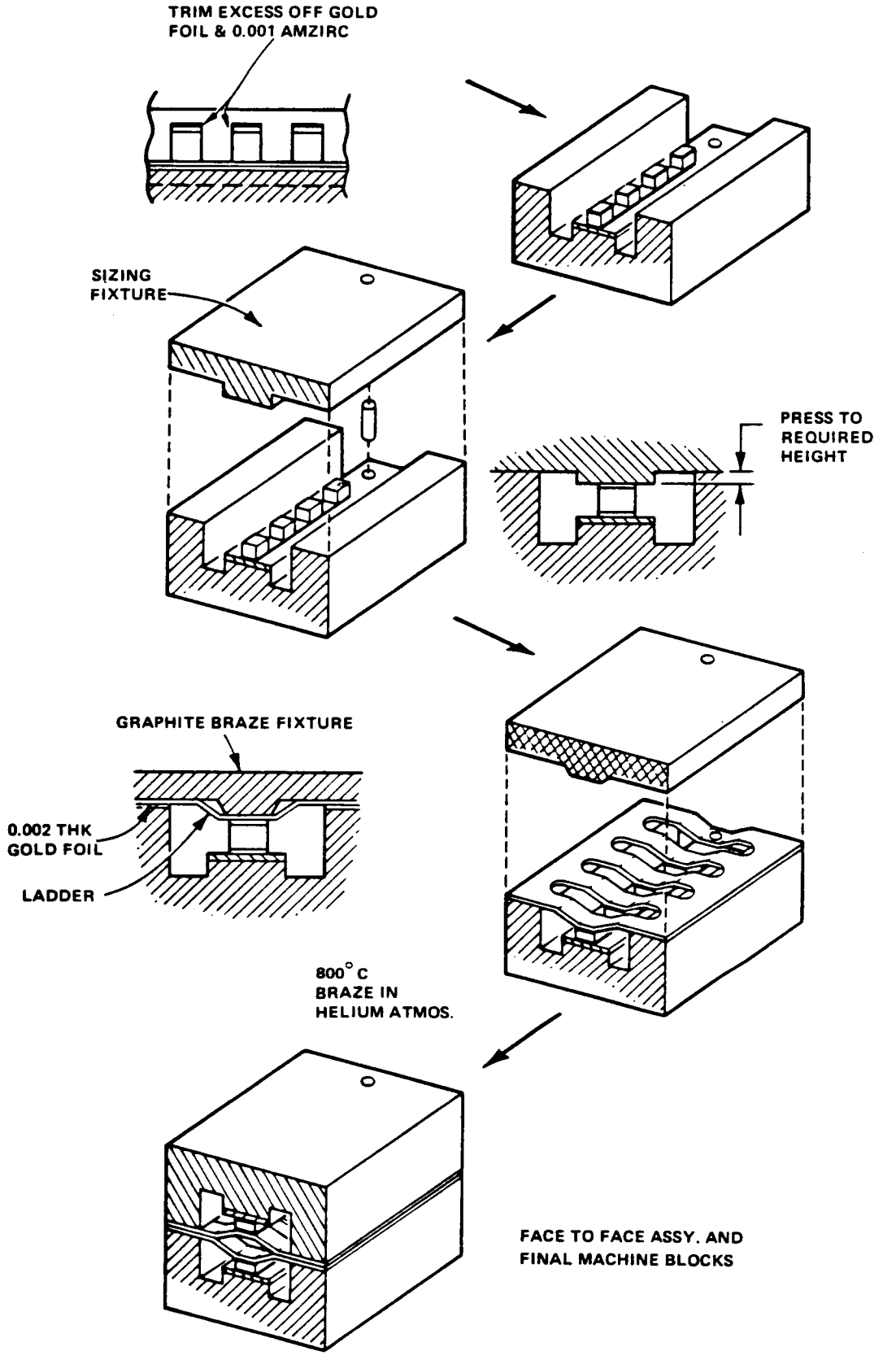

FIGURE 32. ASSEMBLY PROCEDURE THROUGH MATING OF THE TWO FINAL-MACHINED HALVES

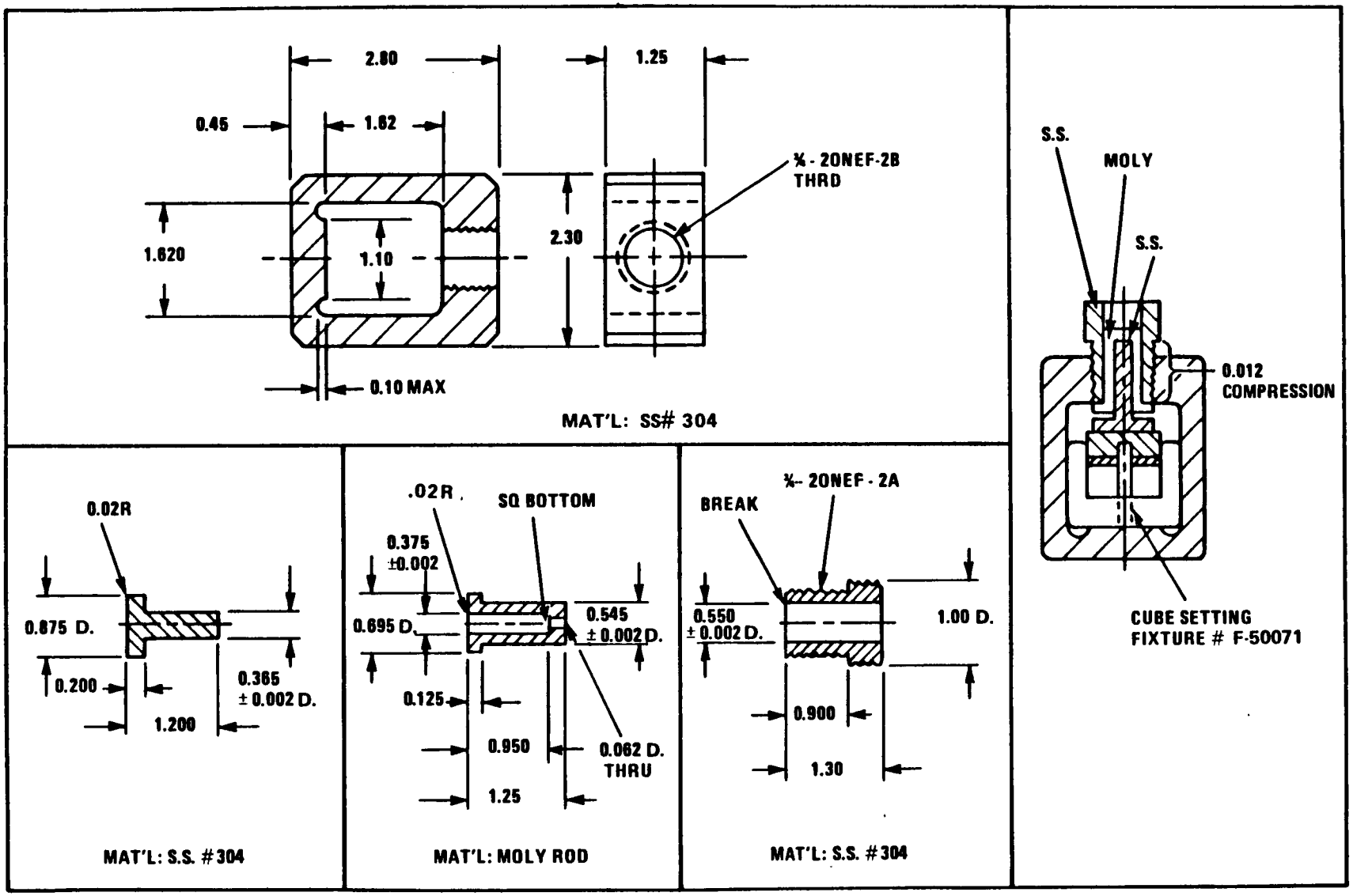

FIGURE 33. BRAZE FIXTURE

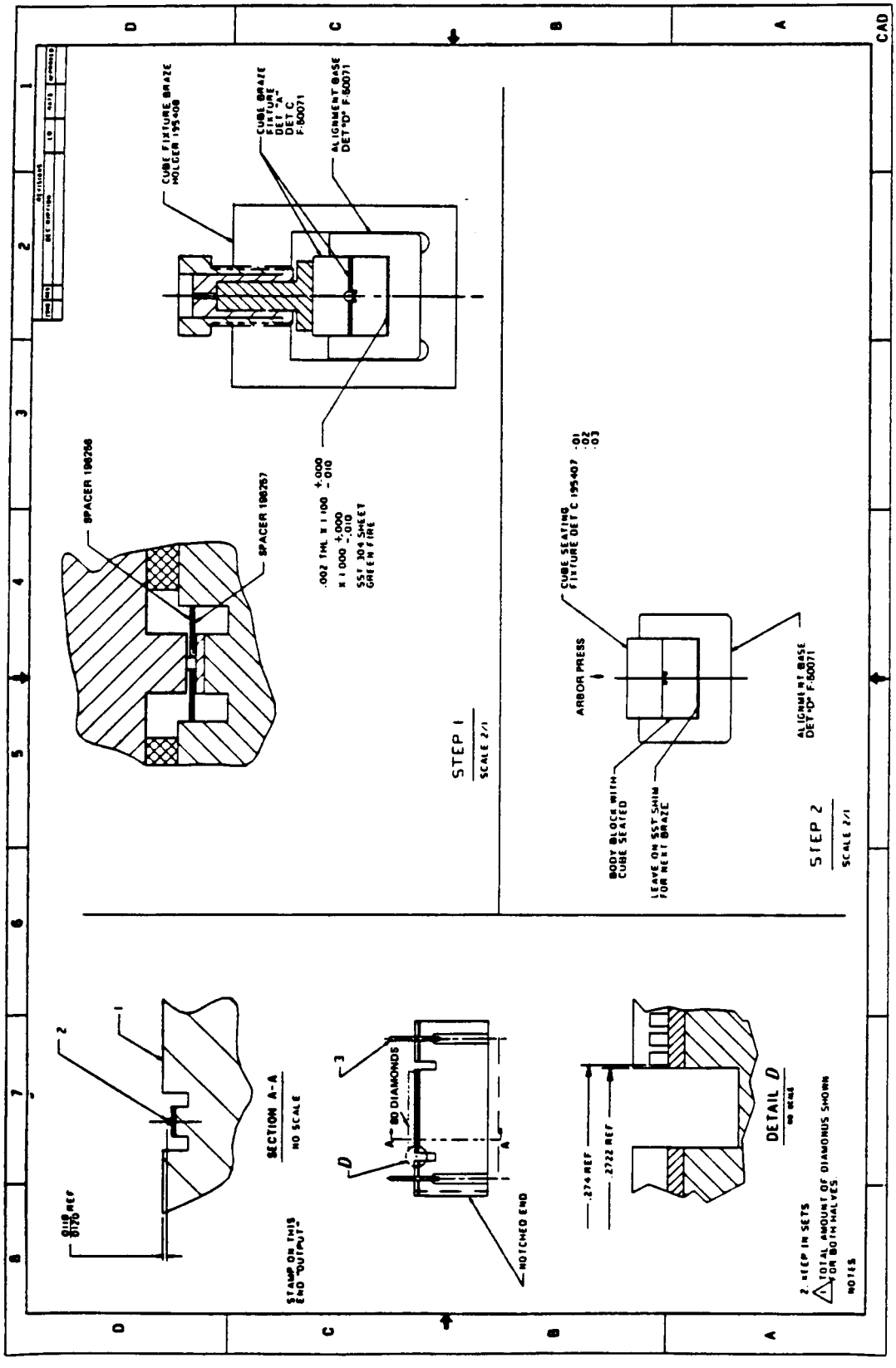

FIGURE 34. ASSEMBLY DRAWING OF DIAMOND BRAZE TO RIDGE ASSEMBLY

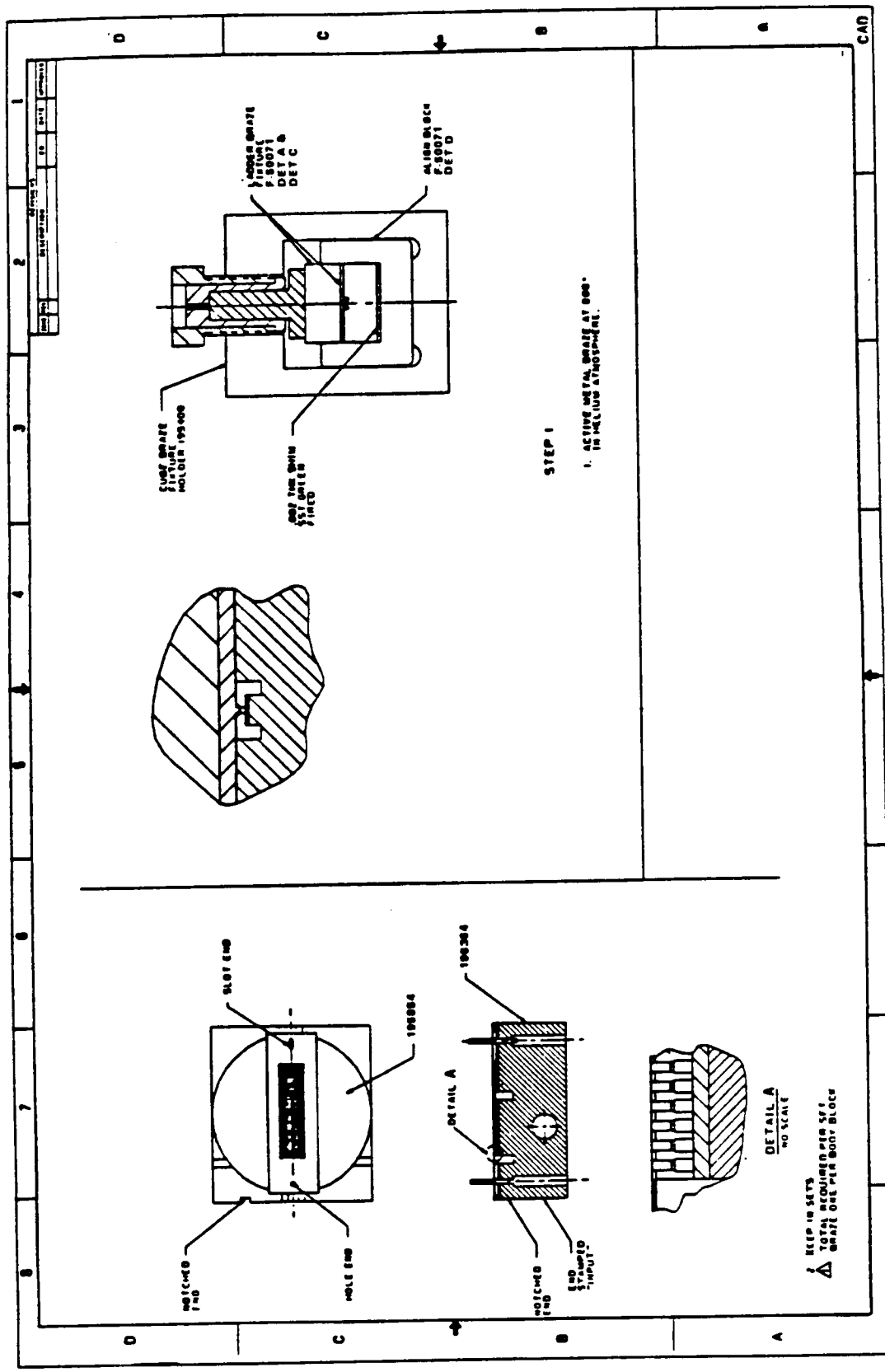

FIGURE 35. ASSEMBLY DRAWING OF BRAZE OF LADDER TO RIDGE-DIAMOND ASSEMBLY

Figure 35 outlines the procedure for brazing the ladder element to the diamonds as well as the ridge block. Shown are the details of the ladder element, the ridged block and the fixtures necessary for brazing at 800°C in helium.

The final braze on these circuit assemblies differs from the earlier designs in two important respects. First, the waveguide assemblies are no longer actually brazed in place. They are held in place with screws, as described in Section 3.3. The waveguide/body contact surface has also been reduced from two planes to one plane. Secondly, the water connections are not brazed in, but are welded in place in final assembly. Both of these changes reduce the complexity of the braze, with resultant increase in reliability.

The work on refining the brazing techniques has reached the point that several low-band circuit assembly brazes have now been successfully made. There were no final high-band circuit assemblies completed, but there was a successful braze on a row of 80 diamonds brazed to a circuit ridge. This braze demonstrated the effectiveness of the brazing fixtures in accounting for differences in expansion coefficient in the various materials used in the circuit assembly, as a row of 80 diamonds is exactly 1.000 inch long. This compares with 0.525 inch which was the longest braze made previously.

4.4 COLLECTOR DESIGN

The collector designed for this program is the same as the collector used on earlier TunneLadder programs. It has a single, depressable stage, and uses conventional assembly techniques for depressed collectors built at Varian. The most important feature of these collectors is a region, backfilled with a combination of stable gases, which vastly increases the resistance to arcing across the heat conduction ceramics. A cross section of the collector is shown in Figure 36.

4.5 WINDOW/WAVEGUIDE DESIGNS

Initially, there were two window designs, namely a low-power, broadband design for the input, and a narrower-band, but proven high-power design for the output. Layouts for each design are shown in Figure 37.

The mechanical construction provides a rugged, mechanically straight-forward assembly, highly resistant to thermal shock or to fracturing. Cold-test results for the input

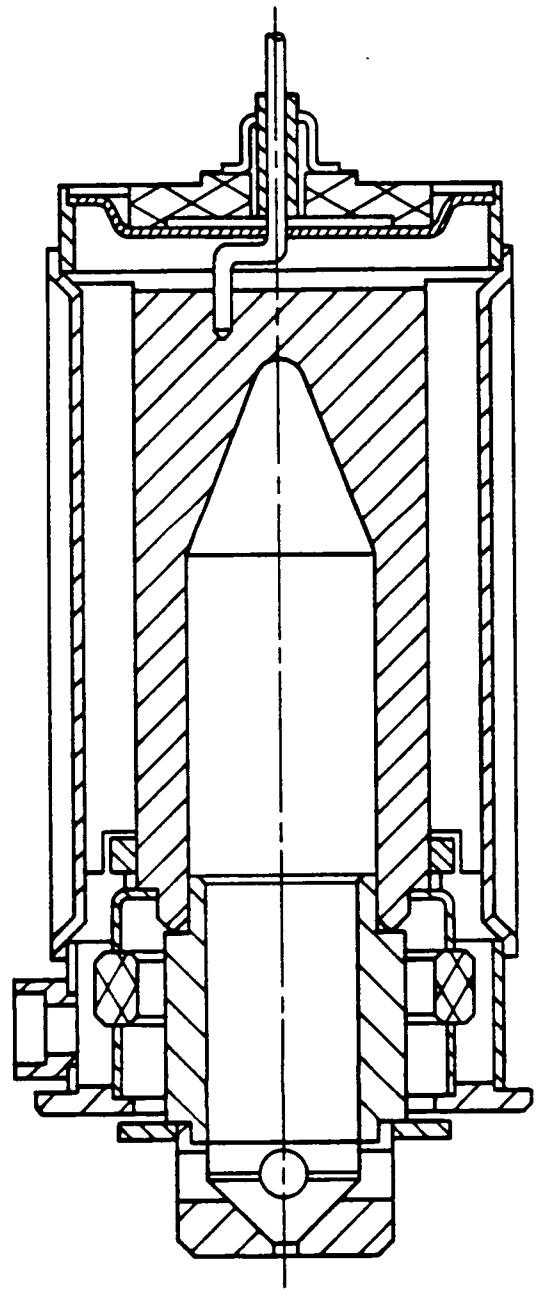

FIGURE 36. COLLECTOR CROSS SECTION

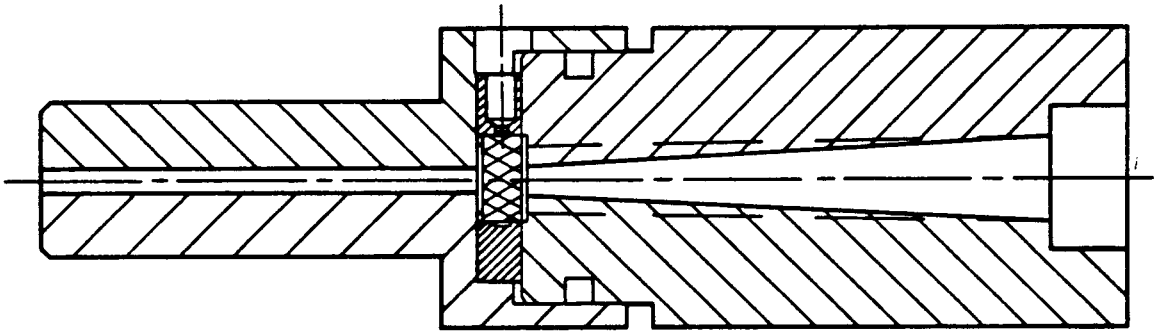

INPUT

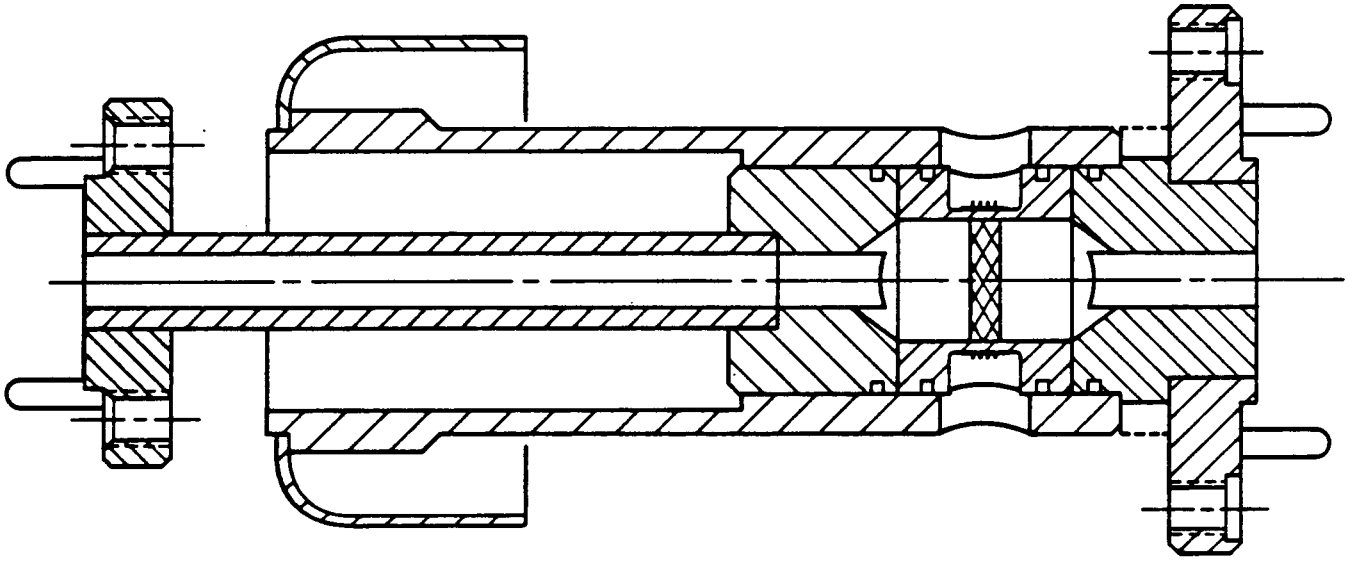

OUTPUT

FIGURE 37. WINDOW DESIGNS

window are shown in Figure 38 and results for the output window are shown in Figure 39. Despite its excellent match performance, the input window design was eventually set aside, and the output design was used at all four ports. This decision was made after we observed that the WR-22 waveguide being used was subject to nonmetallic inclusions of considerable length. Should a small vacuum leak occur in one of the input windows, it would be difficult or impossible to repair. Therefore, the output window, while less well matched, has a far smaller likelihood of compromising tube reliability.

4.6 BODY DESIGN

Figure 40 shows a layout of the completed tube vacuum assembly. In addition to the assemblies described above (i.e., circuit input and output, gun, input and output pole piece, window/waveguide, and collector), there are many other assemblies that are necessary to satisfy thermal and mechanical requirements. Two of these, the anode and "tail pipe" assemblies, furnish liquid-cooled beam drift regions on either end of the circuit assemblies, to protect the thermally fragile circuit elements from potential intercepting beam electrons. The drift tube diameter in these regions is 0.025 inch or about the same dimension as the closest spacing of the ladder elements around the beam hole. There are five cooling tube assemblies, which conduct cooling liquid from the output pole piece (through which the tube cooling inlet and outlet pipes pass) to other major tube subassemblies. Finally, there is an outer shell assembly that serves both as a structural support member and as a major part of the vacuum envelope. In addition to these assemblies, there are a number of brackets and supports, which provide mechanical support to various fragile assemblies. The overall body design approach is aimed toward meeting all of the electrical, mechanical, and thermal requirements with a structure that is easier to assemble and more reliable than those used on the earlier TunneLadder tubes. The body design will then be scaled for use on the 29 GHz TunneLadder tubes.

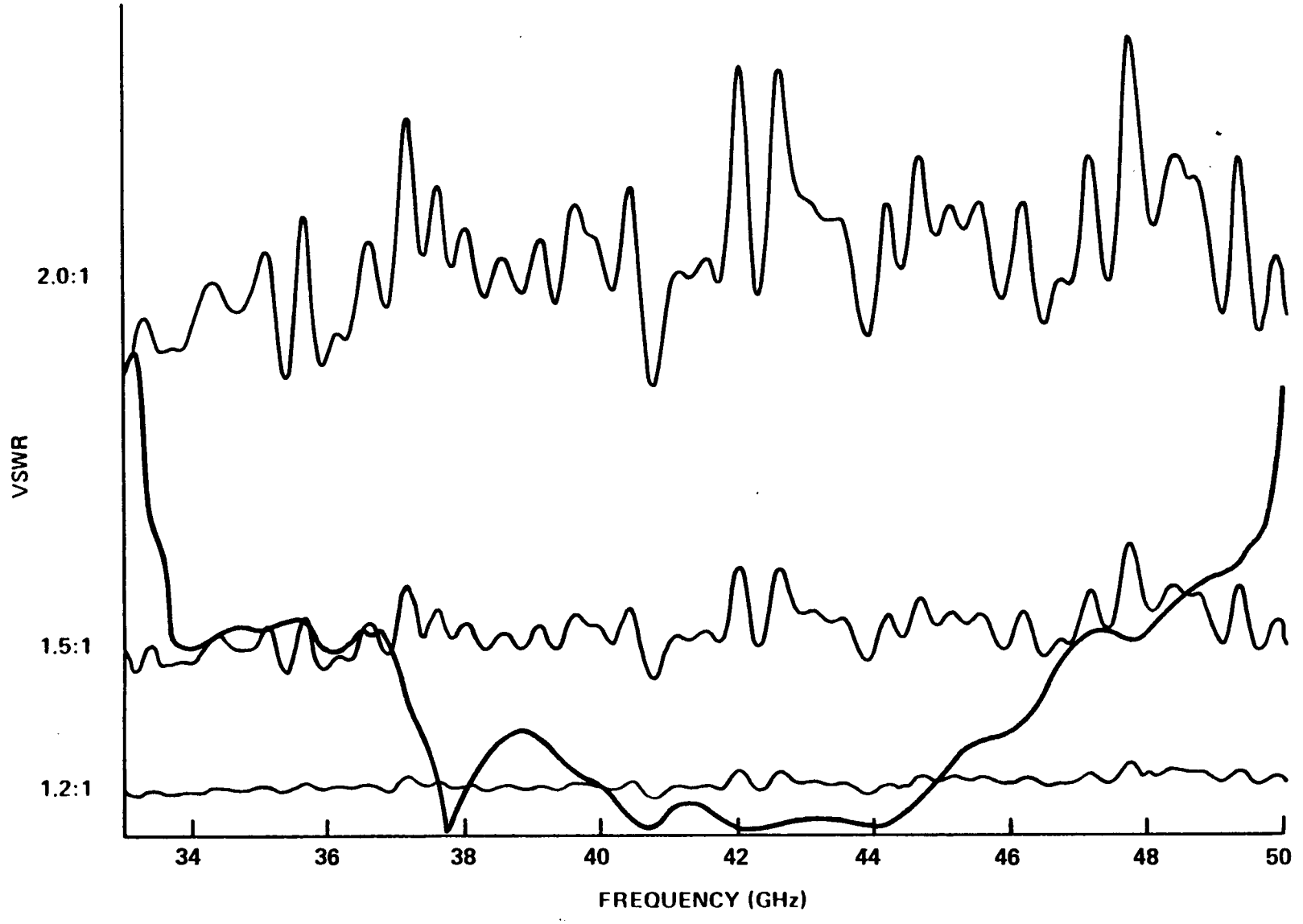

FIGURE 38. INPUT WINDOW MATCH

D2656
F1118

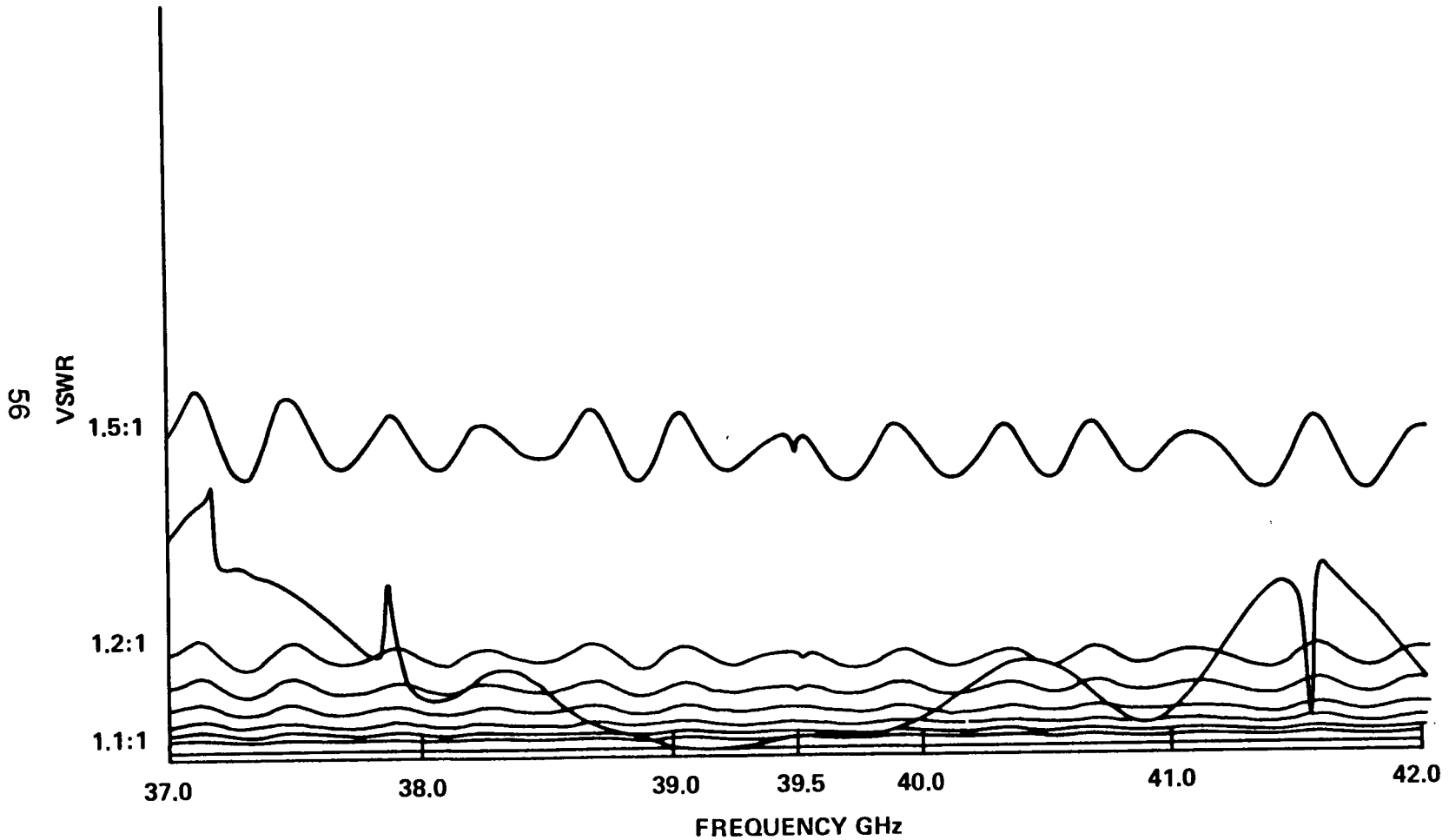

FIGURE 39. OUTPUT WINDOW MATCH

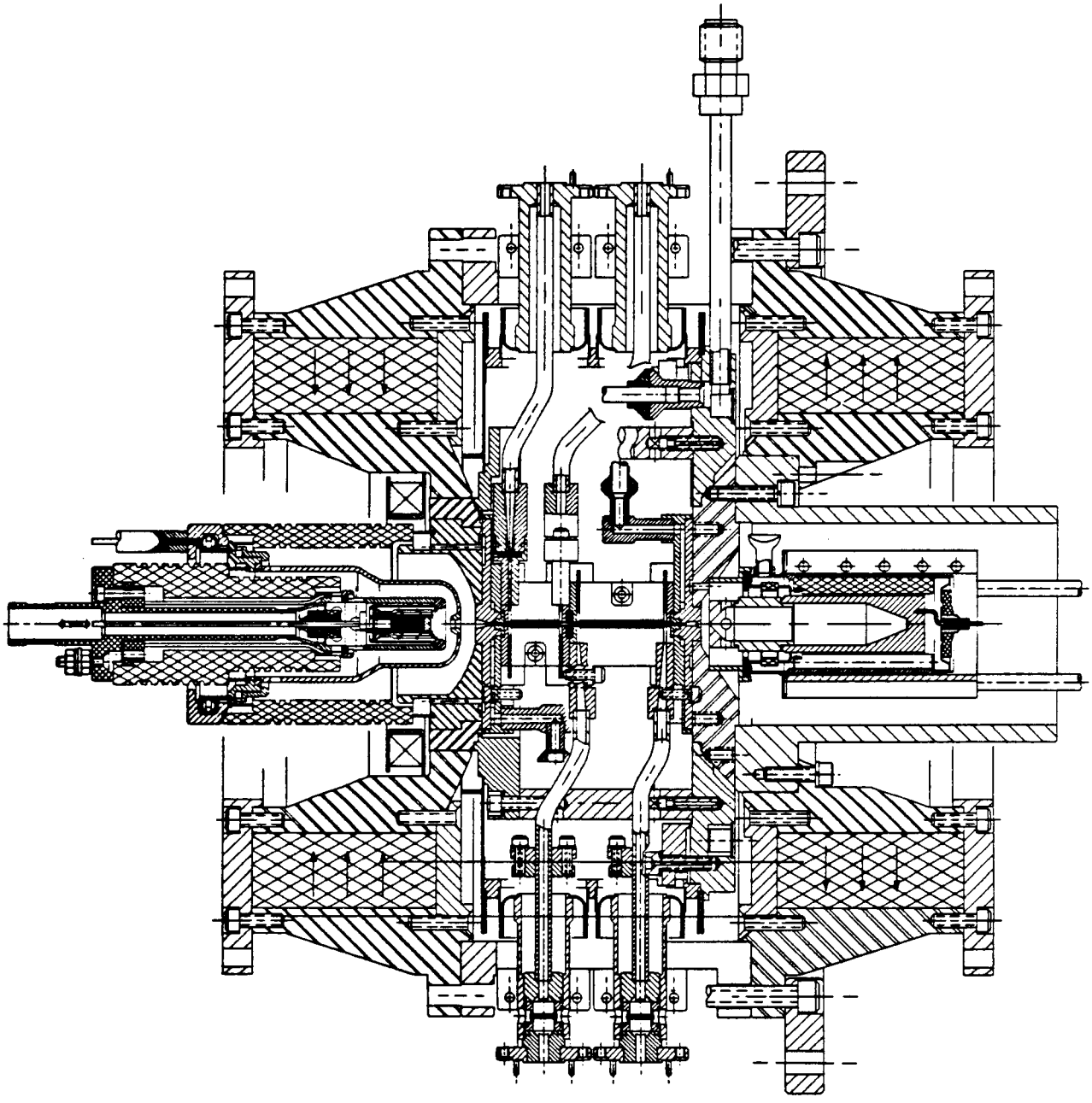

FIGURE 40. VTQ-6299A1 TUBE LAYOUT

5.0 TUBE FABRICATION

Although an entire tube was not completed, several tube assemblies were built, and a number of fabrication problems were uncovered and solved.

5.1 GENERAL OBSERVATIONS

Figure 41a, 41b and 41c are flow charts for a 39.5 GHz TunneLadder TWT. With them one can gain a clear picture of the subassemblies used in the tube, along with the manner in which they are assembled. Those assemblies that are underlined were completed during the course of the program. They have been "bagged" and are stored in an argon atmosphere.

5.2 CIRCUIT

Most information relevant to circuit fabrication is in Sections 3.1, 3.2, and 4.3. Several sets of circuit brazes have now been made successfully on both this program and on the other TunneLadder programs. The culminating activity on this program was the successful brazing of a row of 80 diamonds to a ridge, as described in Section 4.3. The longest entire section brazed on any TunneLadder program has 42 diamonds on each side. Four such assemblies have been made.

5.3 PROBLEMS/SOLUTIONS

The problems associated with tube fabrication conform to no particular pattern. On the contrary, the discussion below simply gives an indication of the great variety of potential failure modes which inevitably arise in a new type of device.

The diamond spacing fixtures are copper strips, 0.002 inch thick, with 100 slots (one for each diamond) and associated locating holes, all with tolerances of 0.0005 inch or less. The slots are photoetched, just as the circuit elements are, and therefore their tolerances are compatible with their fabrication method. However, when one attempts to inspect the parts, problems arise. First, it is difficult to set up an automatic measuring technique from a hole. A flat surface or straight edge would be preferable, but these surfaces are not critical and too expensive to hold to close tolerance. The internal configuration of each slot can be verified by eye, but a systematic method for "reading" each slot automatically is not apparent. Finally, when one attempts to make measurements, using an optical device, the heat from the light

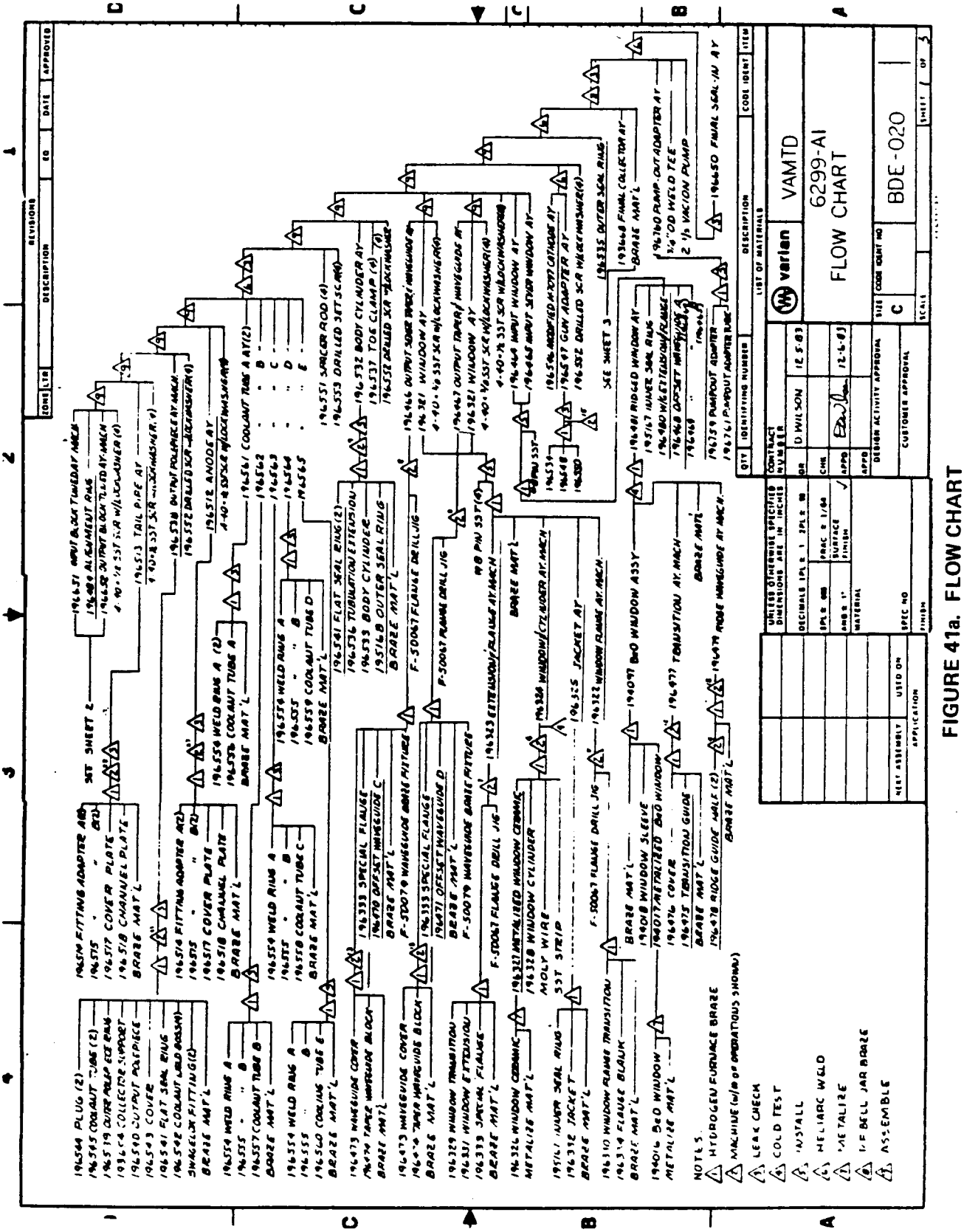

FIGURE 41a. FLOW CHART

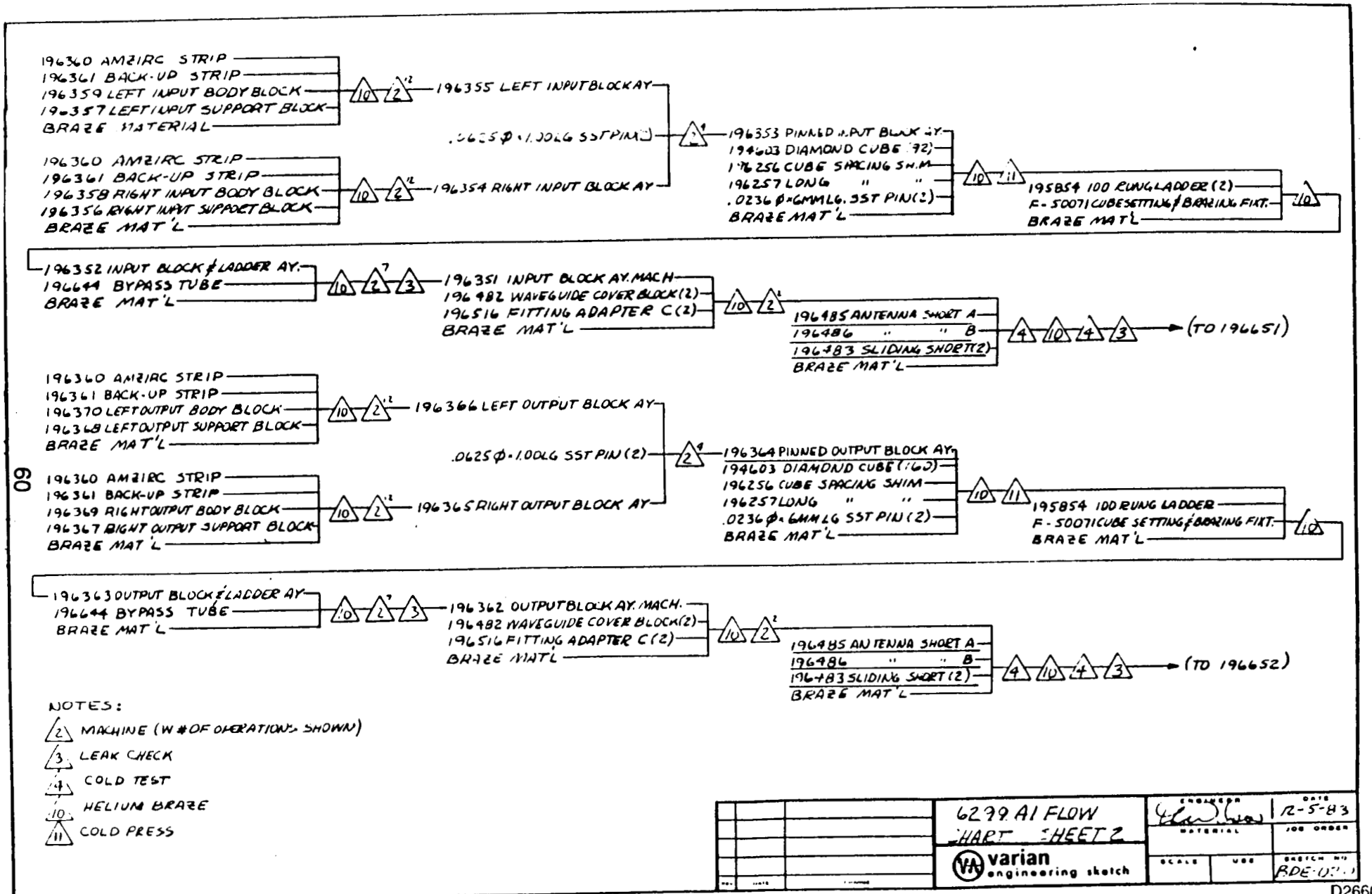

FIGURE 41b. FLOW CHART

D2660
F1118

ORIGINAL PAGE IS
OF POOR QUALITY

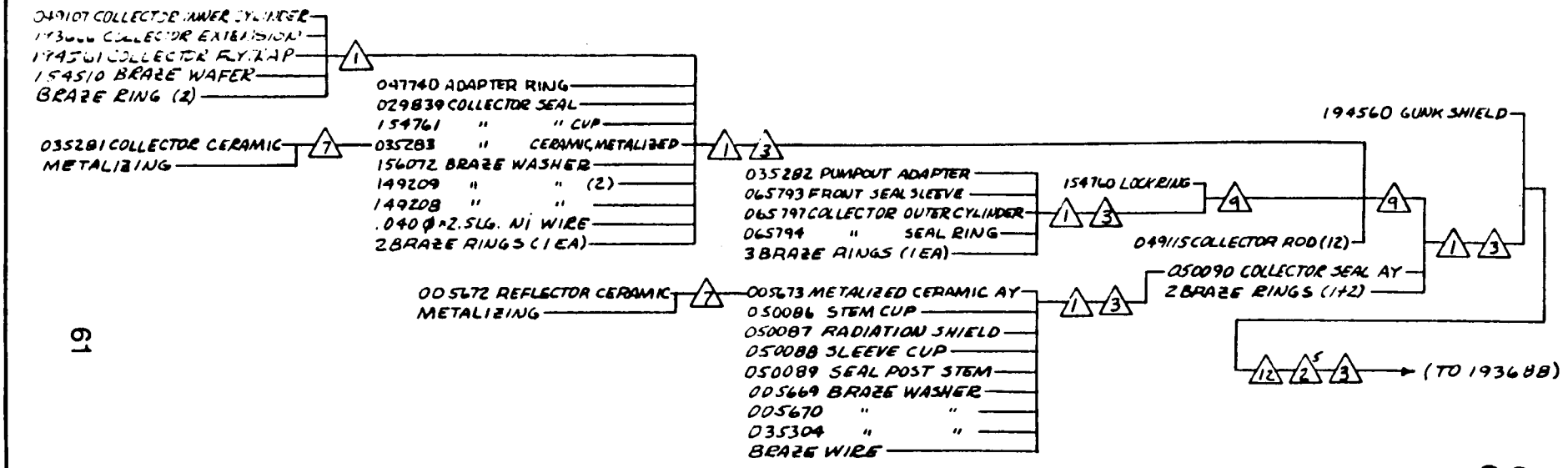

61

NOTES:

1. HYDROGEN FURNACE BRAZE
2. MACHINE (W # OF OPERATIONS SHOWN)
3. LEAK CHECK
7. METALIZE
9. ASSEMBLE
12. LASER WELD

6299 A1 FLOW CHART SHEET 3

varian engineering sketch

ENGINEER L.W. Coon DATE 12-5-83

MATERIAL JOB ORDER

SCALE USE SKETCH NO. BDE-920

FIGURE 41c. FLOW CHART

used to illuminate the part being measured causes the latter to warp, thus putting it out of focus. Nonetheless, through a combination of manual and computer generated measurements, it was possible to verify the conformance of the fixtures to their required tolerances.

Another problem arose when the circuit's outer dimensions were being machined. A chamfer was cut in one wall, with approximately 0.010 x 0.020 inch dimensions. In many applications, such an error would not affect performance, and could be overlooked. However, in this case, the effect would possibly have been to compromise the thermal capability of the circuit. Repairing the circuit was accomplished by machining out the wall in question, and brazing in a small strip of copper, which could then be remachined to the proper dimensions and configuration.

A third problem concerned finding vendors with sufficient skill to deliver acceptable parts in a reasonable time. The photoetched parts and fixtures are the best example of this. Only one vendor consistently provided acceptable parts, while others eitner bid on parts they could not make, or were unable to meet delivery dates.

Finally, one brazed assembly had to be reworked when an angle on a piece part was cut to 42° instead of 48°. Since the angle was close to 45°, and the tolerances of the affected dimensions had not been tight enough, the error was not detected until after the assembly was brazed. However, a second assembly, using correctly dimensioned parts, was brazed successfully.

6.0 CONCLUSIONS/RECOMMENDATIONS

6.1 CONCLUSIONS

On the basis of the work performed on this program, the following conclusions can be reached:

— Scale model cold test fixtures can be used with confidence to predict circuit performance at higher frequencies. In the case of the Karp slow-wave circuit, cold tests done on this and other similar programs indicate that the version of this circuit known as the "TunneLadder" has a variety of potential applications over a wide range of frequencies and voltages.

— Several innovative fabrication techniques can be used successfully in the design of a TunneLadder TWT. In particular, the bonding of copper circuit elements to diamond supports in a feasible approach to providing effective mechanical support and good cooling for TunneLadder circuit elements.

— A rugged, reliable tube can be designed to generate 200 W CW at 39.5 GHz, over a 1.5 to 2% frequency band. However, while such a device might be produced at a price similar to a comparable coupled-cavity TWT, helix and staggered-ladder TWTs with similar performance characteristics are less expensive, and are already built in limited quantities.

— Fabrication of a TunneLadder TWT indicates that a large number of details must be resolved before a manufacturable device is available. These details include inspection and tolerancing, as well as fabrication of piece parts, and eliminating ambiguous assembly techniques.

6.2 RECOMMENDATIONS

As indicated above, considerable work remains to be done to bring the present design up to manufacturable standards. Much of this effort could be accomplished, however, on the 29 GHz tubes built concurrently by Varian under NASA Contract NAS3-23347. In addition, several alternative approaches to TunneLadder tube design could be investigated toward the

end of producing a device more compatible with space-borne operation. These approaches are described in brief below.

One such approach is the design of a PPM-focused structure. Enough field is available with state-of-the-art samarium cobalt magnets to provide adequate focusing. Circuit fabrication would be more difficult, but the existing circuit cross section and ladder design could be incorporated into a PPM stack.

A variety of collector designs could be investigated to improve overall tube efficiency. Again, this type of work was to be investigated on contract NAS3-23347, but that investigation was not intended to be exhaustive.

If PM-focusing is to be retained, several modifications could be attempted to reduce the size and weight of the magnets and pole pieces. The use of higher energy product magnetic material is a possibility. For example, samarium cobalt material with an energy product as high as 30×10^6 gauss-oersteds may soon be available. Also, neodynium-iron, with an even higher energy product, might be useful if its poor thermal properties could be either overcome or compensated for. Another approach to a smaller focusing structure would be to reduce the pole piece-to-pole piece gap, which is now 2.5 inches. Incorporating the pole pieces into the anode and tail pipe assemblies might be an avenue worth exploring.

Other possible improvements would include further investigation of circuit materials, design of internal sever terminations, and a simpler cooling system.

7.0 REFERENCES

1. A. Karp, "Traveling-Wave Tube Experiments at Millimeter Wavelengths with a New, Easily Built, Space-Harmonic Circuit," Proc. I.R.E., vol. 43, pp. 41 - 46 (1955).

2. H. Kosmahl, R. Palmer, "Harmonic-Analysis Approach to the 'TunneLadder': Modified Karp Circuit for Millimeter-Wave TWTAs," IEEE Trans. Electron Devices, vol. ED-29, pp. 862-869, May 1982.

3. A. Karp, "Design Concepts for a High-Impedance Narrow-Band 42 GHz Power TWT Using a 'Fundamental/Forward' Ladder-Based Circuit," Final Report, Varian Associates, Palo Alto, CA, February 1981 (NASCR-165282).

4. A. Karp, "Millimeter-Wave Values," pp. 73 - 128 in Fortschritte der Hochfrequenztechnik, vol. 5, M. Strutt et al., eds., Academic Press MBH, Frankfurt/Main, 1960.

5. Ibid., Fig. 30 (d), p. 116.

6. Ibid., Fig. 30 (e), p. 116.

7. Ibid., bibliography items 118 - 123, p. 127.

8. A. Karp, "Backward-Wave Oscillator Experiments at 100 to 200 Kilomegacycles," Proc. I.R.E., vol. 45, pp. 496 - 503 (1975).

9. L.D. Cohen, "Backward-Wave Oscillators for the 50- to 300-GHz Frequency Range," IEEE Trans. Electron Devices, vol. ED-15, pp. 403 - 404, June 1968.

10. See Reference 4, Fig. 30 (c), (f) and (h), p. 116.

11. Ibid, bibliography items 130a, 131, p. 127.

12. J.R. Pierce, Traveling-Wave Tubes, D. Van Nostrand Co., New York, 1950; Figure 5.7, p. 90.

13. J.R. Pierce, "Propagation in Linear Arrays of Parallel Wires," I.R.E. Trans. Electron Devices, vol. ED-2, pp. 13 - 24, (1955).

14. See Reference 4, bibliography items 125, 127, 128, p. 127.

15. H.G. Kosmahl and T. O'Malley, "Harmonic Analysis of the Forward-Wave Karp Circuit as a Millimeter-Wave Amplifier in the 100 - 500 W Range," Microwave Power Tube Conference, Monterey, CA, 3 May 1978.

16. A. Jacquez, A. Karp, D. Wilson, and A. Scott, "A Millimeter-Wave Tunneladder TWT," Final Report for NASA Contract NAS3-22466, July 1984.

NASA
National Aeronautics and Space Administration

Report Documentation Page

1. Report No.	2. Government Accession No.	3. Recipient's Catalog No.
CR 182182		

4. Title and Subtitle
Development of a 39.5 GHz Karp Traveling Wave Tube for use in Space - Final Report

5. Report Date

6. Performing Organization Code

7. Author(s)
A. Jacquez and D. Wilson

8. Performing Organization Report No.

10. Work Unit No.
506-61-42

9. Performing Organization Name and Address
Varian Associates
Microwave Tube Division
611 Hansen Way
Palo Alto, CA 94303

11. Contract or Grant No.
NAS 3-23259

13. Type of Report and Period Covered
Final Report
Jan 1981 - July 1984

12. Sponsoring Agency Name and Address
Lewis Research Center
21000 Brookpark Road
Cleveland, OH 44135

14. Sponsoring Agency Code

15. Supplementary Notes
Lewis Research Center Contract Manager,
James A. Dayton, Jr., Space Electronics Division

16. Abstract

A millimeter-wave TWT was developed using a dispersive, high-impedance forward wave interaction structure based on a ladder, with non-space-harmonic interaction, for a tube with high gain per inch and high efficiency. The "TunneLadder" interaction structure combines ladder properties modified to accommodate Pierce gun beam optics in a radially magnetized PM focusing structure. The development involved the fabrication of chemically milled, shaped ladders diffusion brazed to diamond cubes which are in turn active-diffusion brazed to each ridge of a doubly ridged waveguide.

Cold-test data are presented, representing the $\omega\beta$ and impedance characteristics of the modified ladder circuit. These results were used in small and large-signal computer programs to predict TWT gain and efficiency.

A laboratory model tube was designed and fabricated, including all major subassemblies.

17. Key Words (Suggested by Author(s))	18. Distribution Statement
Traveling Wave Tube Tunneladder Fundamental Wave Structure Diamond Supports	Publicly Available

19. Security Classif. (of this report)	20. Security Classif. (of this page)	21. No of pages	22. Price*

NASA FORM 1626 OCT 86

*For sale by the National Technical Information Service, Springfield, Virginia 22161